Redox Biology 38 (2021) 101757

Contents lists available at ScienceDirect

Redox Biology

journal homepage: www.elsevier.com/locate/redox

Research Paper

Targeting feed-forward signaling of TGFβ/NOX4/DHFR/eNOS uncoupling/TGFβ axis with anti-TGFβ and folic acid attenuates formation of aortic aneurysms: Novel mechanisms and therapeutics

Kai Huang [1], Yongchen Wang [1], Kin Lung Siu [1], Yixuan Zhang, Hua Cai [*]

Division of Molecular Medicine, Department of Anesthesiology, Division of Cardiology, Department of Medicine, David Geffen School of Medicine, University of California Los Angeles, Los Angeles, CA, 90095, USA

ARTICLE INFO

Keywords:
NADPH oxidase (NOX)
NOX isoform 4 (NOX4)
Reactive oxygen species (ROS)
eNOS uncoupling/recoupling
Thoracic aortic aneurysm (TAA)
Marfan syndrome (MFS)
Abdominal aortic aneurysm (AAA)
Folic acid (FA)
Transforming growth factor–β (TGFβ)
Tetrahydrobiopterin (H_4B)
Dihydrofolate reductase (DHFR)
Nitric oxide (NO)
GTP cyclohydrolase 1 (GTPCHI)

ABSTRACT

In the present study we aimed to identify novel mechanisms and therapeutics for thoracic aortic aneurysm (TAA) in *Fbn1*$^{C1039G/+}$ Marfan Syndrome (MFS) mice. The expression of mature/active TGFβ and its downstream effector NOX4 were upregulated while tetrahydrobiopterin (H_4B) salvage enzyme dihydrofolate reductase (DHFR) was downregulated in *Fbn1*$^{C1039G/+}$ mice. In vivo treatment with anti-TGFβ completely attenuated NOX4 expression, restored DHFR protein abundance, reduced ROS production, recoupled eNOS and attenuated aneurysm formation. Intriguingly, oral administration with folic acid (FA) to recouple eNOS markedly alleviated expansion of aortic roots and abdominal aortas in *Fbn1*$^{C1039G/+}$ mice, which was attributed to substantially upregulated DHFR expression and activity in the endothelium to restore tissue and circulating levels of H_4B. Notably, circulating H_4B levels were accurately predictive of tissue H_4B bioavailability, and negatively associated with expansion of aortic roots, indicating a novel biomarker role of circulating H_4B for TAA. Furthermore, FA diet abrogated TGFβ and NOX4 expression, disrupting the feed-forward loop to inactivate TGFβ/NOX4/DHFR/eNOS uncoupling axis in vivo and in vitro, while PTIO, a NO scavenger, reversed this effect in cultured human aortic endothelial cells (HAECs). Besides, expression of the rate limiting H_4B synthetic enzyme GTP cyclohydrolase 1 (GTPCHI), was downregulated in *Fbn1*$^{C1039G/+}$ mice at baseline. In cultured HAECs, RNAi inhibition of fibrillin resulted in reduced GTPCHI expression, while this response was abrogated by anti-TGFβ, indicating TGFβ-dependent downregulation of GTPCHI in response to fibrillin deficiency. Taken together, our data for the first time reveal that uncoupled eNOS plays a central role in TAA formation, while anti-TGFβ and FA diet robustly abolish aneurysm formation via inactivation of a novel TGFβ/NOX4/DHFR/eNOS uncoupling/TGFβ feed-forward pathway. Correction of fibrillin deficiency is additionally beneficial via preservation of GTPCHI function.

1. Introduction

Aortic aneurysms are associated with high morbidity and mortality, accounting for more than 200,000 deaths each year worldwide [1]. In the United States, approximately 16,950 patients die of ruptured aneurysms annually [1]. Aneurysmal disease in humans has hereditary influence, particularly for thoracic aortic aneurysm (TAA) [2], although non-genetic factors also play important roles in aneurysm development and progression [3–6]. Hereditary thoracic aortic aneurysm and dissection (HTAAD) includes Marfan syndrome (MFS), Loeys-Dietz syndrome and other HTAAD conditions. It has been established that fibrillin-1 (*FBN1*) mutation is the cause of aneurysm formation in patients with MFS [2]. Fibrillin-1 is the main component of 10 nm microfibrils and serves as a skeleton to provide anchoring and load-bearing functions within the arterial wall [7], deficiency of which impairs extracellular matrix (ECM) integrity leading to aneurysm formation [2]. Nonetheless, molecular mechanisms underlying TAA formation in MFS or other non-genetic conditions have remained incompletely understood.

TGFβ and its related pathways have been implicated in the

* Corresponding author. Division of Molecular Medicine, Department of Anesthesiology, Division of Cardiology, Department of Medicine, David Geffen School of Medicine, University of California Los Angeles, 650 Charles E Young Dr., Los Angeles, CA, USA.
E-mail address: hcai@mednet.ucla.edu (H. Cai).
[1] The authors contribute equally to this work.

https://doi.org/10.1016/j.redox.2020.101757
Received 13 July 2020; Received in revised form 29 August 2020; Accepted 8 October 2020
Available online 13 October 2020

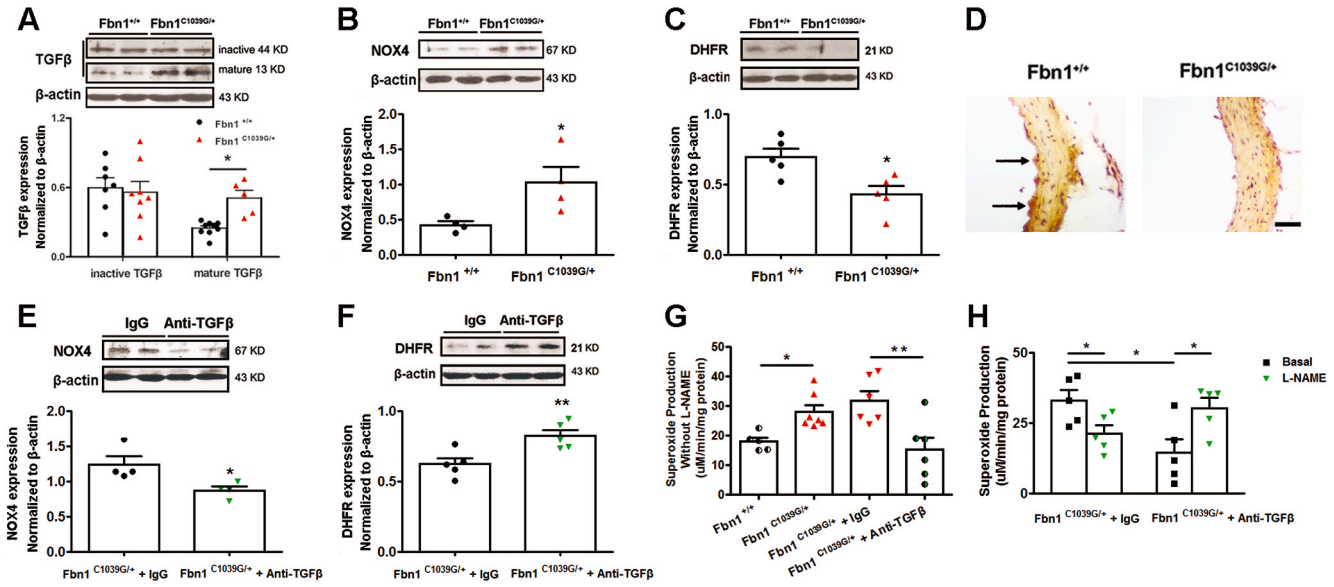

Fig. 1. TGFβ blocking antibody recouples eNOS and attenuates ROS production via inhibition of NOX4 and restoration of DHFR expression in *Fbn1*$^{C1039G/+}$ mice. The aortas were isolated from 12 weeks old *Fbn1*$^{+/+}$ and *Fbn1*$^{C1039G/+}$ mice and subjected to Western blotting, immunohistochemistry (IHC) and electron spin resonance (ESR) analyses. **(A)** Representative Western blots and grouped densitometric data of aortic protein expression levels of inactive and mature TGFβ indicating upregulation of mature TGFβ in *Fbn1*$^{C1039G/+}$ mice. Data are presented as Mean ± SEM, n = 5–9. **(B)** Representative Western blots and grouped densitometric data of aortic NOX4 protein expression indicating upregulation of NOX4 in *Fbn1*$^{C1039G/+}$ mice. Data are presented as Mean ± SEM, n = 4. **(C)** Representative Western blots and grouped densitometric data of endothelial DHFR protein expression indicating downregulation of DHFR in *Fbn1*$^{C1039G/+}$ mice. Data are presented as Mean ± SEM, n = 5. **(D)** Representative IHC images of aortic roots, indicating downregulation of endothelial DHFR in 12 weeks *Fbn1*$^{C1039G/+}$ mice. Arrows indicating highly expressed DHFR in the endothelial layer of the control animals, which was however reduced in *Fbn1*$^{C1039G/+}$ mice. In parallel experiments, 4 weeks old *Fbn1*$^{C1039G/+}$ mice were treated with TGFβ blocking antibody for 4 weeks prior to analyses of NOX4 expression and eNOS uncoupling activity. **(E)** Representative Western blots and grouped densitometric data of aortic NOX4 protein expression in *Fbn1*$^{C1039G/+}$ mice treated with TGFβ blocking antibody, indicating abrogated NOX4 expression. Data are presented as Mean ± SEM, n = 4. **(F)** Representative Western blots and grouped densitometric data of endothelial DHFR protein expression in *Fbn1*$^{C1039G/+}$ mice treated with TGFβ blocking antibody, indicating restored DHFR expression. Data are presented as Mean ± SEM, n = 5. **G)** Superoxide production was determined by ESR in the aortic tissues of *Fbn1*$^{C1039G/+}$ mice after TGFβ blocking antibody treatment for 4 weeks. The results indicate that TGFβ blocking antibody reduced ROS production. Data are presented as Mean ± SEM, n = 5–7. **(H)** Total superoxide production in the presence or absence of L-NAME was determined by ESR in the aortic tissues of *Fbn1*$^{C1039G/+}$ mice after TGFβ blocking antibody treatment for 4 weeks. The results indicate recoupling of eNOS by treatment with TGFβ blocking antibody. Data are presented as Mean ± SEM, n = 5. Bar = 30 μm, *p < 0.05, **p < 0.01.

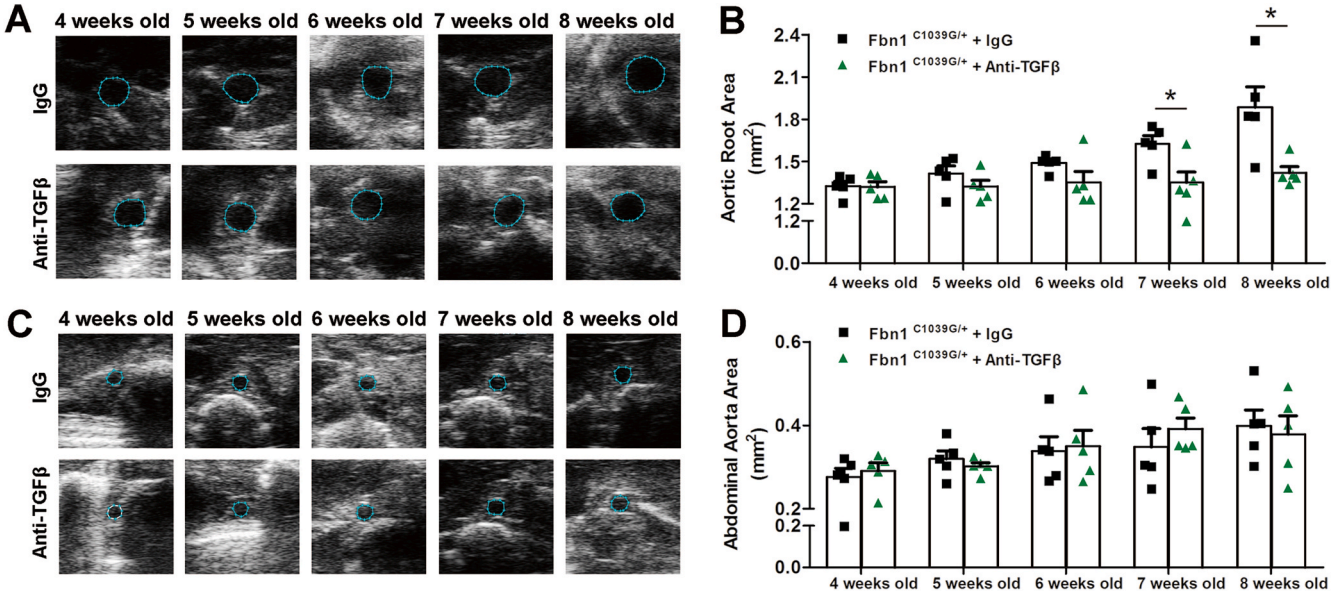

Fig. 2. TGFβ blocking antibody attenuates aortic root expansion via inhibition of NOX4-uncoupled eNOS axis in *Fbn1*$^{C1039G/+}$ mice. Four weeks old *Fbn1*$^{C1039G/+}$ mice were treated with TGFβ blocking antibody for 4 weeks to analyze expansion of aortic roots and abdominal aortas. **(A)** Representative images of aortic root expansion detected by echocardiography. **(B)** Echo-defined areas of aortic root areas were attenuated by treatment with TGFβ blocking antibody for 3 or 4 weeks in *Fbn1*$^{C1039G/+}$ mice. **(C)** Representative images of abdominal aorta expansion detected by echocardiography. **(D)** Echo-defined areas of abdominal aorta were yet changed after treatment with TGFβ blocking antibody for 4 weeks in *Fbn1*$^{C1039G/+}$ mice, likely attributed to slower progression of AAA in *Fbn1*$^{C1039G/+}$ mice. Data are presented as Mean ± SEM, n = 5. *p < 0.05.

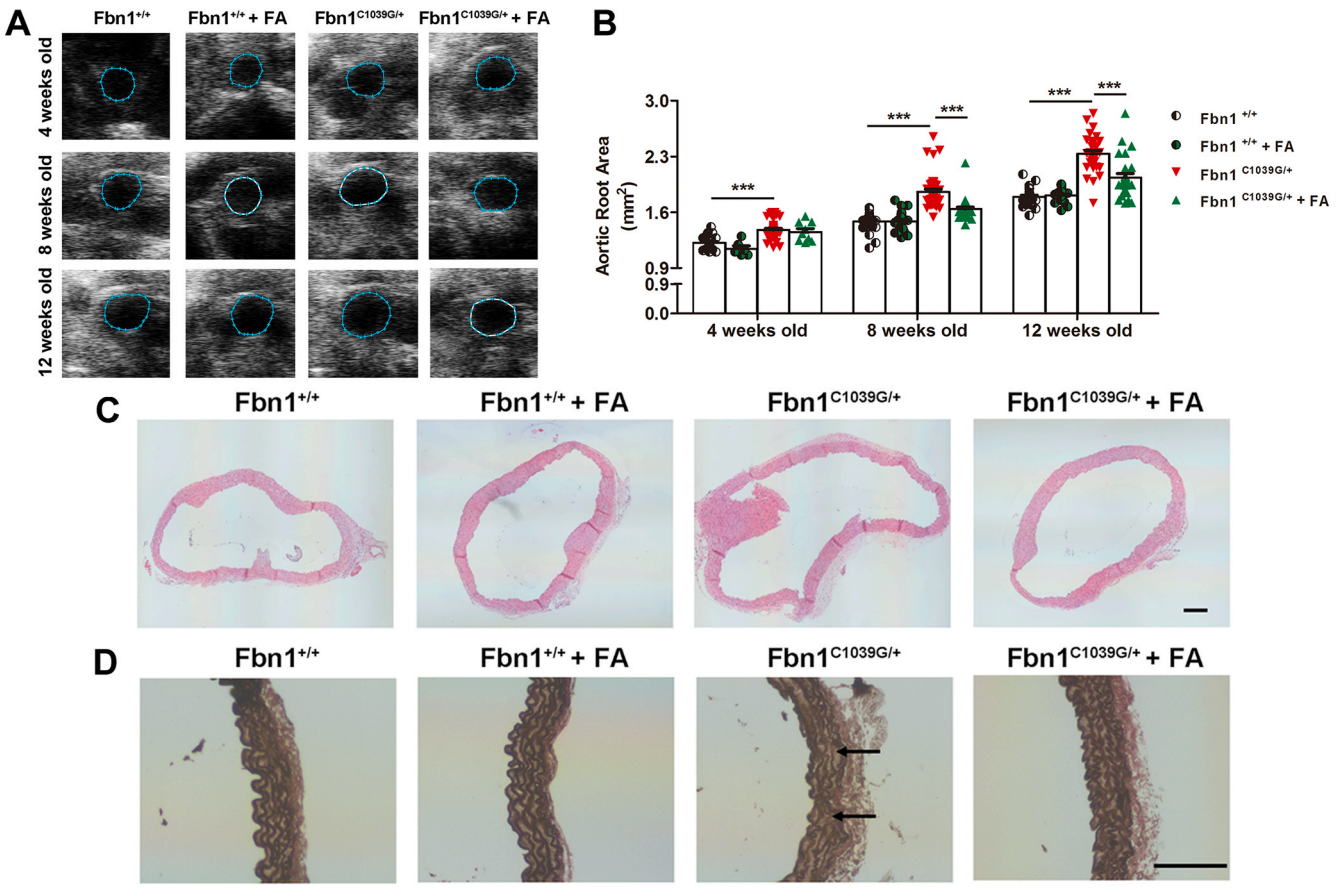

Fig. 3. Recoupling of eNOS with folic acid diet abrogates expansion of aortic roots in *Fbn1*$^{C1039G/+}$ animals. *Fbn1*$^{+/+}$ and *Fbn1*$^{C1039G/+}$ mice of 4 weeks age were fed FA diet (15 mg/kg/day) for 4 and 8 weeks. **(A)** Representative images of aortic roots by echocardiography. **(B)** Echo-defined areas of aortic roots indicating time-dependent expansion of aortic roots in *Fbn1*$^{C1039G/+}$ mice, which was attenuated by FA diet. Data are presented as Mean ± SEM, n = 6–41. **(C)** Representative Hematoxylin-Eosin (H&E) images of aortic roots, indicating features of expansion and remodeling in *Fbn1*$^{C1039G/+}$ mice that were alleviated by FA diet. **(D)** Representative Verhoeff-Van Gieson (VVG) images of aortic roots. Arrows indicate flattening and degradation of elastin fibers, which were attenuated by FA diet. Bar = 100 μm, ***$p < 0.001$.

pathogenesis of TAA formation in MFS [2]. However, the precise roles and mechanisms of TGFβ signaling in TAA formation have remained controversial [8–10]. TGFβ signaling and noncanonical (smad-independent) TGFβ signaling both drive aneurysm progression in Fbn1$^{C1039G/+}$ strain [11,12], where NOX4 seems to function as a downstream effector [13,14]. However, in the more severe model of Marfan aneurysm (*Fbn1*$^{mgR/mgR}$ mice), TGFβ neutralization either exacerbated or mitigated TAA formation depending on whether treatment was initiated before or after aneurysm formation, respectively [15]; and that a potential role of NOX4 in this model has not been explored. In addition, even in Fbn1$^{C1039G/+}$ strain, the molecular details downstream of NOX4 in the modulation of aneurysm formation, need to be further elucidated. Importantly, we have demonstrated a prominent role of NOX4 induced eNOS uncoupling and ROS production in the pathogenesis of many cardiovascular diseases, including a novel finding in the formation of aneurysm in the abdominal fragment of the aortas [16–22]. Therefore, in the present study we aim to delineate a role of TGFβ/NOX4 axis in activating eNOS uncoupling to mediate TAA formation in MFS mice.

Our recent work has established a direct causal role of uncoupled eNOS and endothelium-derived ROS in AAA formation in both novel and classical models of AAA including Ang II infused hph-1 mice and Ang II infused apoE null mice [18–22]. Endothelial deficiency in DHFR is responsible for eNOS uncoupling to result in sustained oxidative stress, redox-sensitive activation of MMP2 and MMP9, and inflammatory responses of macrophage infiltration, resulting in matrix degradation and AAA formation [18–22]. Furthermore, we have shown that restoration of DHFR expression in the endothelium and recoupling of eNOS with oral administration of folic acid (FA) is remarkably effective in attenuating AAA formation in Ang II-infused hph-1 or apoE null mice [18–22]. Therefore, we tested the hypotheses that eNOS uncoupling is induced by TGFβ-NOX4 axis in MFS mice to result in endothelial dysfunction, sustained oxidative stress and cascaded events to stimulate matrix degradation and aneurysm formation in the aortic roots, and that targeting this novel signaling pathway with anti-TGFβ or FA diet is robustly effective in preventing Marfan aneurysms.

In the present study, we used the classical model of MFS, the fibrillin-1 mutant mice (*Fbn1*$^{C1039G/+}$), to examine novel molecular mechanisms and therapeutics for TAA that are in urgent need for clinical management of the disease, since no oral medicine is available to treat this fatal and devastating disease except for surgical correction with considerable risk. Indeed, we identified a novel, feed-forward mechanism of TGFβ/NOX4/DHFR/eNOS uncoupling/TGFβ axis in the development of TAA in MFS mice, targeting of which with anti-TGFβ or FA diet (via DHFR/H_4B/eNOS recoupling/NO pathway) abrogates aneurysm formation. Notably, FA diet downregulated TGFβ and NOX4 protein expression, further inactivating the signaling axis that leads to aneurysm formation; and this response is NO-dependent. Correction of fibrillin is additionally beneficial in preserving the rate limiting H_4B synthetic enzyme GTP cyclohydrolase 1 (GTPCHI) function to maintain eNOS coupling activity.

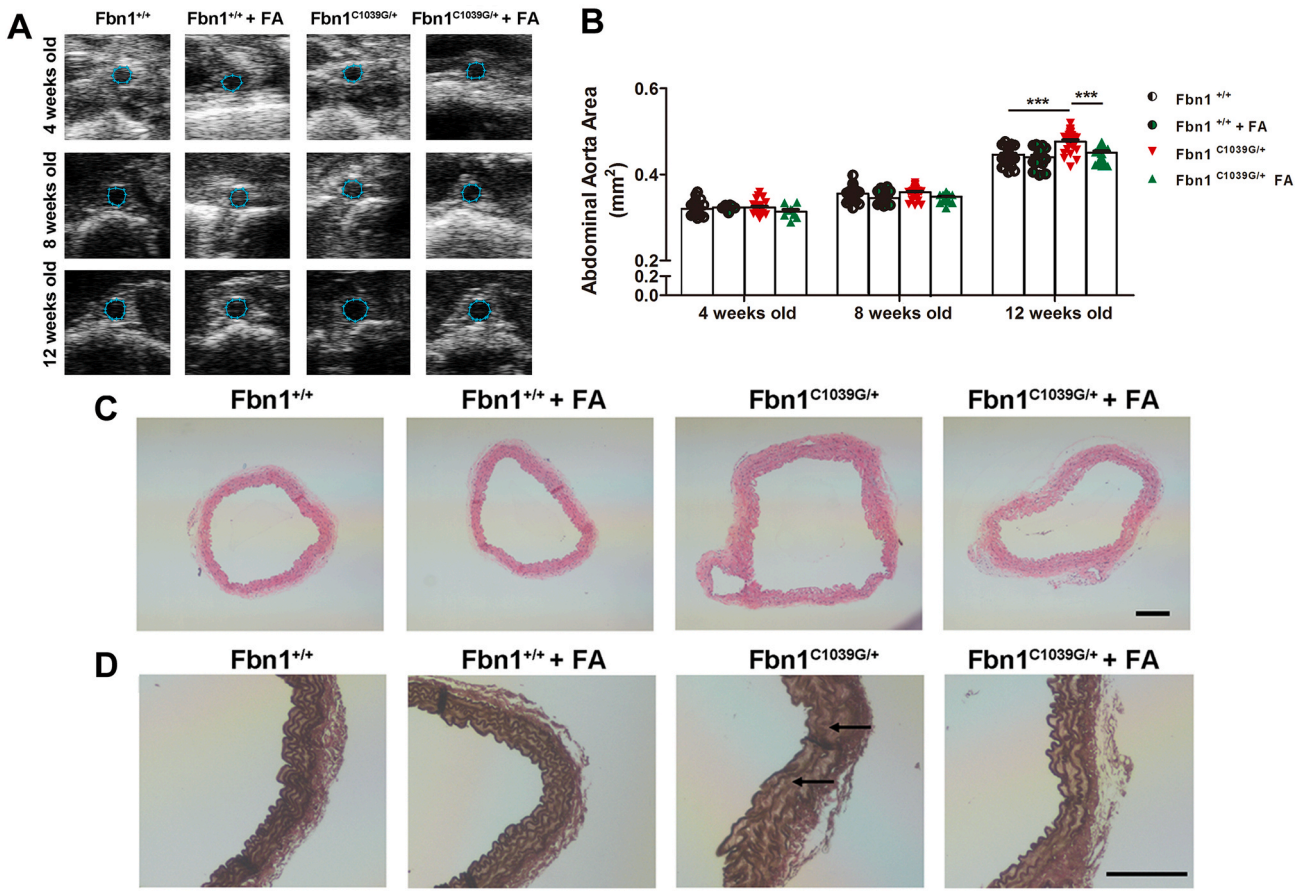

Fig. 4. Recoupling of eNOS with folic acid diet abrogates expansion of abdominal aortas in *Fbn1*$^{C1039G/+}$ animals. *Fbn1*$^{+/+}$ and *Fbn1*$^{C1039G/+}$ mice of 4 weeks age were fed FA diet (15 mg/kg/day) for 4 and 8 weeks. **(A)** Representative images of abdominal aortas by echocardiography. **(B)** Echo-defined areas of abdominal aortas indicating time-dependent expansion of abdominal aortas in *Fbn1*$^{C1039G/+}$ mice, which was attenuated by FA diet. Data are presented as Mean ± SEM, n = 6–38. **(C)** Representative H&E images of abdominal aortas, indicating features of expansion and remodeling in *Fbn1*$^{C1039G/+}$ mice that were alleviated by FA diet. **(D)** Representative VVG images of abdominal aortas. Arrows indicate flattening and degradation of elastin fibers, which were attenuated by FA diet. Bar = 100 μm, ***p < 0.001.

2. Methods

2.1. Animals

Animal experiments were performed according to the approval by the Institutional Animal Care and Usage committee at the University of California, Los Angeles (UCLA). The breeding founders of heterozygous *Fbn1*$^{C1039G/+}$ male mice were purchased from Jackson Labs (Bar Harbor, ME, Strain B6.129-*Fbn1*^{tm1Hcd}/J, stock#012885). The animals develop proximal aortic aneurysms, mitral valve thickenings, pulmonary alveolar septation defects, mild thoracic kyphosis, and skeletal myopathy, but 90% reportedly live to one year of age [11]. The animals have been previously backcrossed into C57BL/6 background [11]. All pups were genotyped using PCR (Supplemental Fig. 1) following instructions from Jackson Labs. Since the incidence of thoracic aortic disease (including aneurysm and dissection) is higher in men than in women [23,24], male mice have been used for experimentation.

2.2. In vivo and in vitro treatment with anti-TGFβ antibody

Four weeks old heterozygous *Fbn1*$^{C1039G/+}$ male animals were treated with TGFβ neutralizing antibody (anti-TGFβ, clone 1D11, Bio X Cell) or isotype (IgG, clone MOPC21, Bio X Cell) as previously shown [25]. One mg anti-TGFβ or isotype reagent was injected intraperitoneally on the first day, and then 200 μg was injected intraperitoneally every other day for 13 times. The ultrasound imaging of aortic root and the abdominal aorta were performed every week as described below. Aortic superoxide production and eNOS uncoupling activity were determined after 4 weeks injection as described below.

For in vitro experiments, male origin human aortic endothelial cells (HAECs) were isolated from male donor after obtaining permission for research applications by informed consent (Lonza, Walkersville, MD, USA). HAECs were cultured in EGM-2 media (EBM-2 basal medium with supplement pack, all reagents from Lonza (Walkersville, MD, USA). Cells of passages 4 to 6 were starved in EBM-2 basal medium overnight and then treated with 20 μg/mL anti-TGFβ (clone 1D11, Bio X Cell, West Lebanon, NH, USA) or IgG (clone MOPC21, Bio X Cell) for 24 h, prior to determination of protein expression levels of GTPCHI using Western blotting.

2.3. Isolation of endothelial cells from aorta

Endothelial cells (ECs) were isolated from aortas as we previously described [18,20–22,26]. In brief, freshly isolated aortas were cut into small sections (~2 mm) and digested in PBS containing collagenase (0.6 mg/mL) for 20 min at 37°C. The aortic rings were then gently shaken in the digestion buffer to remove ECs. The ECs were collected via centrifugation at 1,000*g* for 3 min at 4 °C. Both the denuded rings and ECs were lysed with lysis buffer for subsequent analyses.

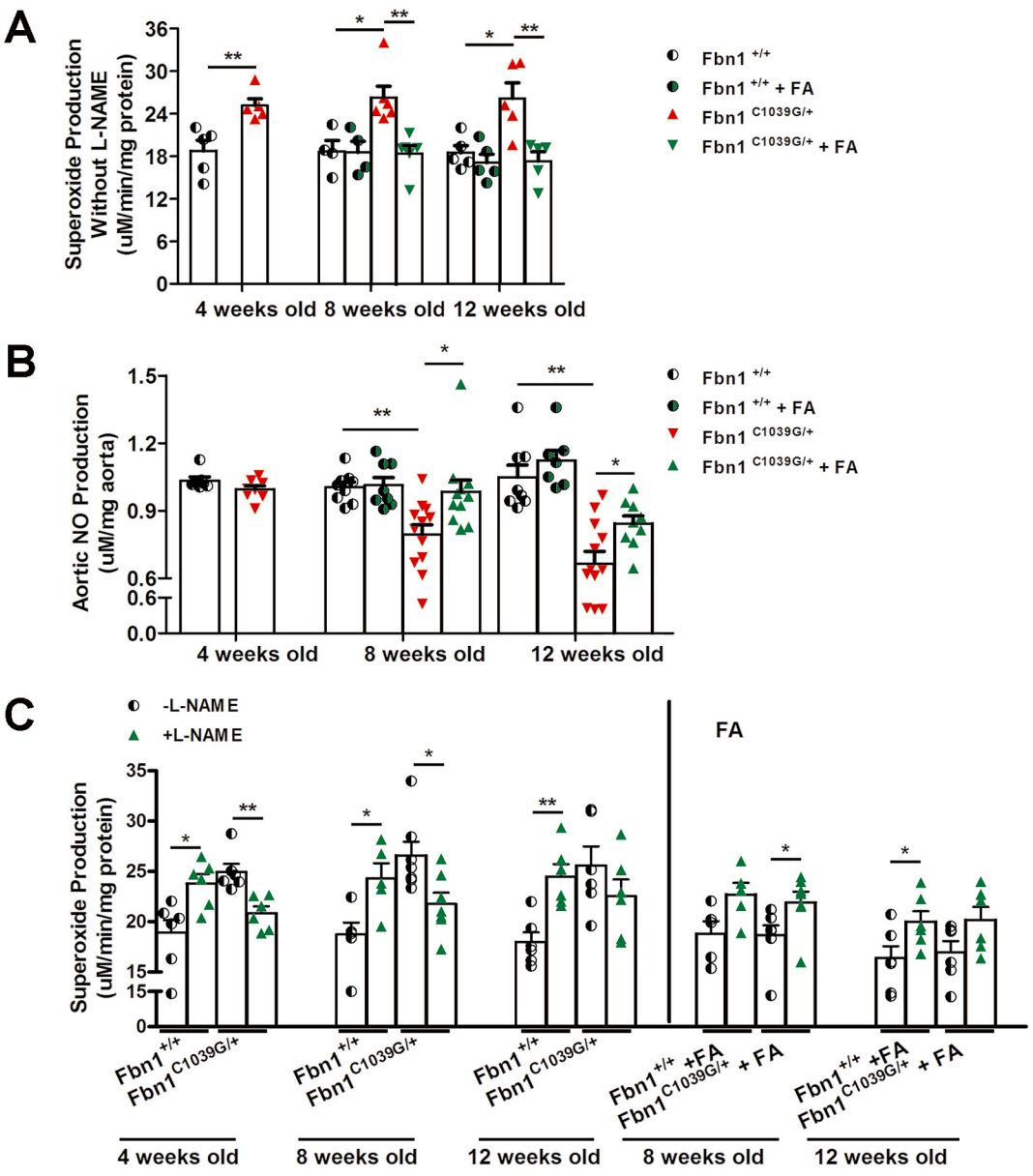

Fig. 5. Folic acid diet reduces superoxide production, restores NO bioavailability and recouples eNOS in *Fbn1*$^{C1039G/+}$ mice. *Fbn1*$^{+/+}$ and *Fbn1*$^{C1039G/+}$ mice of 4 weeks age were fed FA diet (15 mg/kg/day) for 4 and 8 weeks, after which aortas were freshly harvested for electron spin resonance (ESR) determination of superoxide production, NO bioavailability and eNOS uncoupling activity. **(A)** Superoxide production was significantly elevated at 4, 8 and 12 weeks of age in *Fbn1*$^{C1039G/+}$ mice, which was completely attenuated by FA diet after oral FA administration for 4 and 8 weeks. Data are presented as Mean ± SEM, n = 4–6. **(B)** NO bioavailability was time-dependently decreased at 8 and 12 weeks of age in *Fbn1*$^{C1039G/+}$ mice, which was completely or largely restored by FA diet. Data are presented as Mean ± SEM, n = 7–12. **(C)** Total superoxide production in the presence or absence of L-NAME was measured by ESR for determination of eNOS uncoupling activity (L-NAME-inhibitable superoxide production) in *Fbn1*$^{C1039G/+}$ mice. eNOS was uncoupled at 4, 8 and 12 weeks of age in *Fbn1*$^{C1039G/+}$ mice, which was completely attenuated by FA diet. Data are presented as Mean ± SEM, n = 5–7. *p < 0.05, **p < 0.01.

2.4. Western blotting

Western blotting was performed following standard protocols, using 10–12.5% SDS/PAGE gel and nitrocellulose membranes. Primary antibodies and their dilutions used were: TGFβ (1:500, Abcam, ab92486), NOX4 (1:500, Novus Biologicals, NB110–58849SS), DHFR (1:500, Novus Biologicals, H00001719-M01), eNOS (1:2000, BD Transduction Laboratories, 610297), GTPCHI (1:400, Sigma-Aldrich, SAB1410516), Fibrillin (1:500, Invitrogen, MA5-12770), and β-actin (1:3000, Sigma-Aldrich, A2066). The intensities of protein bands were analyzed and quantified by the NIH Image J software.

2.5. Immunohistochemistry (IHC) staining

The aortas were embedded in optimal cutting temperature (OCT) compound, and then the frozen tissue sections were prepared with Cryostat Microm HM 525 (Thermo Scientific, Walldorf, Germany). Sections were warmed up at room temperature (RT), and incubated in PBST containing 0.1% Triton for 30 min. After incubated in 0.3% H_2O_2 in methanol for 30 min at RT, the sections were washed for 3 times with PBST. Sections were incubated with 5% normal goat serum for 2 h, followed by incubation with DHFR primary antibody (1:100, Novus Biologicals, H00001719-M01) at 4°C overnight. The sections were washed with PBST 3 times before and after being incubated with biotin conjugated anti-mouse secondary antibody (Vecta stain ABC kit, CA,

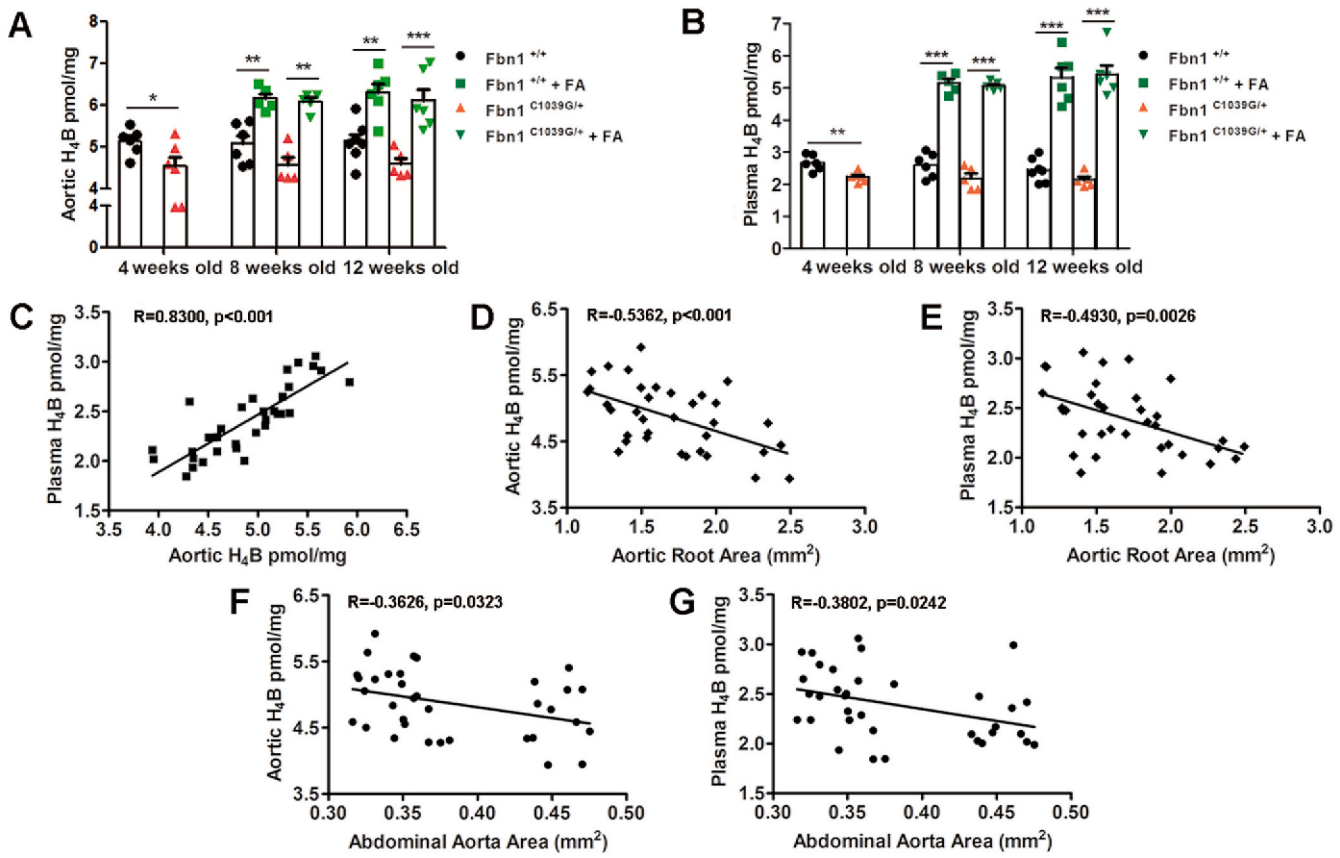

Fig. 6. Folic acid diet restores tissue and circulating H_4B levels in *Fbn1*$^{C1039G/+}$ animals, and a biomarker role of circulating H_4B for TAA. *Fbn1*$^{+/+}$ and *Fbn1*$^{C1039G/+}$ mice of 4 weeks age were fed FA diet (15 mg/kg/day) for 4 and 8 weeks, after which aortas and plasma were freshly collected for HPLC determination of H_4B levels. Aortic H_4B levels **(A)** and plasma H_4B levels **(B)** were determined by HPLC (Data are presented as Mean ± SEM, n = 5–7). FA diet restored tissue and circulating H_4B levels in both wild-type *Fbn1*$^{+/+}$ littermates and *Fbn1*$^{C1039G/+}$ mice. **(C)** Correlation analysis of aortic H_4B and circulating H_4B levels indicating that circulating H_4B is accurately reflective of tissue H_4B levels, R = 0.8300, p < 0.001. n = 35. **(D)** Correlation between aortic root areas and aortic H_4B levels indicating that lower tissue H_4B levels are associated with bigger expansion of aortic roots, R = −0.5362, p < 0.001. n = 35. **(E)** Correlation between aortic root areas and plasma H_4B levels indicating that lower circulating H_4B levels are associated with bigger expansion of aortic roots, R = −0.4930, p = 0.0026. n = 35. **(F)** Correlation between abdominal aorta areas and aortic H_4B levels indicating that lower tissue H_4B levels are associated with bigger expansion of abdominal aortas, R = −0.3626, p = 0.0323. n = 35. **(G)** Correlation between abdominal aorta areas and plasma H_4B levels indicating that lower circulating H_4B levels are associated with bigger expansion of abdominal aortas, R = −0.3802, p = 0.0242. n = 35.

USA). The sections were then incubated in PBST containing reagent A and B (A:B:PBST = 3:3:94, Vecta stain ABC kit, CA, USA) for 2 h at RT. After incubation, the sections were washed 3 times and developed with DAB substrate (D3939, Sigma, USA). The sections were then counter-stained with hematoxylin and dehydrated in 95% and 100% alcohol, and finally washed in xylene. After drying, the sections were mounted with Permount (Fisher Scientific, Pittsburgh, PA, USA) and imaged using a Nikon Eclipse TE2000-U microscope.

2.6. Determination of superoxide production and eNOS uncoupling activity using electron spin resonance (ESR)

Aortic superoxide production was determined by electron spin resonance (ESR) as we previously described [18,19,21,22,26–33]. In brief, freshly isolated aortas were homogenized on ice in lysis buffer containing 1:100 protease inhibitor cocktail, and centrifuged at 12,000*g* for 15 min. Protein contents of the supernatants were determined using a protein assay kit (Bio-Rad, #500–0113, #500–0114, #500–0115). Five μg of protein was mixed with ice-cold and nitrogen bubbled Krebs/HEPES buffer containing diethyldithiocarbamic acid (5 μmol/L), deferoxamine (25 μmol/L), and the superoxide specific spin trap methoxycarbonyl-2,2,5,5-tetramethylpyrrolidine (CMH, 500 μmol/L, Axxora, San Diego, CA, USA). The mixture was then loaded into a glass capillary (Kimble, Dover, OH, USA), and assayed using the ESR spectrometer (eScan, Bruker, Billerica, MA, USA) for superoxide production. A second measurement was taken with the addition of PEG-SOD (100 U/mL). For assessment of eNOS uncoupling activity, a third measurement was made with the addition of L-NAME (100 μmol/L). The ESR settings used were: Center field, 3480; Sweep width, 9 G; microwave frequency, 9.78 GHz; microwave power, 21.02 mW; modulation amplitude, 2.47 G; 512 points of resolution; receiver gain, 1000.

2.7. Ultrasound imaging of aortic root and abdominal aorta

Animals were anesthetized with 1.5% isoflurane (Piramal Healthcare) at 2 L/min oxygen flow using a Isoflurane vaporizer (Tec 3 Isoflurane vaporizer), and secured onto a temperature controlled table to maintain temperature at 37°C. Hair from the abdomen and the chest were removed with a hair removal cream (Nair). Preheated ultrasound transmission gel was applied to the chest (for the aortic root) or the abdomen (for the abdominal aorta). An ultrasound probe (Velvo 2100, echocardiograph, MS-400) was placed on the gel to visualize the aorta transversely. For the abdominal aorta, the aorta was first confirmed by the identification of pulsatile flow using Doppler measurements. Consistent localization for image acquisition was insured by imaging the area immediately superior to the branch of the left renal artery. For the aortic root, the aorta that is immediately superior to the heart was

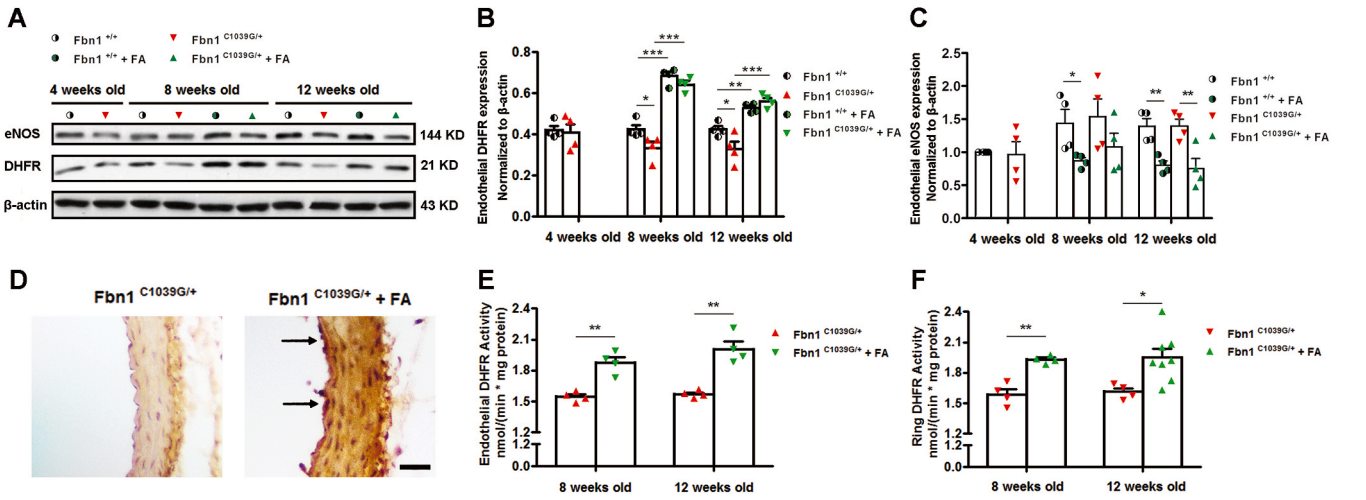

Fig. 7. Folic acid diet restores endothelial DHFR protein expression and activity in *Fbn1*$^{C1039/+}$ mice. *Fbn1*$^{+/+}$ and *Fbn1*$^{C1039G/+}$ mice of 4 weeks age were treated with FA diet (15 mg/kg/day) for 4 and 8 weeks, after which Western blotting was used to examine endothelial DHFR and eNOS expression levels, while IHC was used to detect in situ DHFR protein expression. In parallel experiments, HPLC was used to determine DHFR activity in both isolated aortic endothelial cells (ECs) and the EC-denuded aortas. **(A)** Representative Western blots of endothelial DHFR and eNOS protein expression with β-actin serving as an internal control. **(B)** Grouped densitometric data of endothelial DHFR protein expression, indicating that FA diet upregulated endothelial DHFR protein abundance in both *Fbn1*$^{+/+}$ and *Fbn1*$^{C1039G/+}$ mice. Data are presented as Mean ± SEM, n = 4. **(C)** Grouped densitometric data of eNOS expression, indicating that FA diet decreased endothelial eNOS protein expression in both *Fbn1*$^{+/+}$ and *Fbn1*$^{C1039G/+}$ mice. When uncoupled, upregulation of eNOS represents a deteriorating response, which has been previously shown in apoE null mice and hph-1 mice where eNOS is modestly uncoupled at baseline. Hence, a reduction in eNOS while uncoupled is beneficial on the contrary. Data are presented as Mean ± SEM, n = 4. **(D)** Representative IHC images of aortic roots, indicating upregulation of DHFR protein abundance in 12 weeks *Fbn1*$^{C1039G/+}$ mice fed FA diet. Arrows indicate reduced DHFR expression in the endothelial layer which was however restored by oral FA administration. In parallel experiments, DHFR activity was determined from both isolated ECs. Data are presented as Mean ± SEM, n = 4. **(E)** and the EC-denuded aortas. Data are presented as Mean ± SEM, n = 4–8. **(F),** indicating increased activity in both fractions. However, only the endothelial DHFR activity is relevant to eNOS coupling/uncoupling activity. Bar = 30 μm, *p < 0.05, **p < 0.01, ***p < 0.001.

imaged, and the aorta was confirmed using Doppler measurements. All images were recorded and saved for offline aortic dimension analysis.

2.8. Oral administration of folic acid

The animals were treated with folic acid at 15 mg/kg/day as we previously published [18,19], using customerized food of adding folic acid to standard chow used for control mice. For control mice, standard chow diet (5053-PicoLab Rodent Diet 20, LabDiet, St. Louis, MO) was supplied. FA diet was given to mice at 4 weeks of age, which lasted through the entire study period of 8 weeks till harvest (when mice were 12 weeks old).

2.9. H&E staining and Verhoeff-Van Gieson (VVG) staining

H&E staining was performed by the Translational Pathology Core Laboratory at UCLA following standard protocols. For VVG staining, paraffin embedded tissue sections were de-paraffinized by sequential washes in xylene (2×), descending alcohol from 100% to 50%, then into distilled water. Sections were then stained in Verhoeff's solution for 70 min, followed by differentiation in 2% ferric chloride for 90 s. Sections were incubated with 5% sodium thiosulfate for 60 s, followed by counterstaining with Van Gieson's solution and dehydration in 95% and 100% alcohol, and finally washed in xylene. After drying, the tissues were mounted with Permount (Fisher Scientific, Pittsburgh, PA, USA) and imaged using a Nikon Eclipse TE2000-U microscope.

2.10. Determination of nitric oxide (NO) bioavailability using ESR

Aortic NO bioavailability was determined by ESR as we previously described [18,19,21,22,26–33]. In brief, freshly isolated aortas were cut into 2 mm rings, and then incubated in freshly prepared NO specific spin trap $Fe^{2+}(DETC)_2$ (0.5 mmol/L) in nitrogen bubbled, modified Krebs/HEPES buffer at 37°C for 60 min, in the presence of calcium ionophore A23187 (10 μmol/L). The aortic rings were snap frozen in liquid nitrogen and loaded into a finger Dewar for measurement with ESR spectrophotometer (eScan, Bruker, Billerica, MA, USA). The instrument settings used were as the followings: Center field, 3440; Sweep width, 100 G; microwave frequency, 9.796 GHz; microwave power 13.26 mW; modulation amplitude, 9.82 G; 512 points of resolution; and receiver gain 356.

2.11. Determination of tetrahydrobiopeterin (H_4B) bioavailability using HPLC

Aortic and circulating levels of H_4B were determined using HPLC as we previously described [18,19,21,22,26–29,31–33]. For determination of tissue H_4B bioavailability, freshly isolated aortas were lysed in H_4B lysis buffer (0.1 M phosphoric acid, 1 mM EDTA, 10 mM dl-dithiothreitol) and centrifuged at 12,000*g* for 3 min at 4°C in the dark. For determination of circulating H_4B bioavailability, equal volumes of plasma and H_4B lysis buffer were mixed and incubated on ice for 20 min in the dark and then centrifuged at 12,000*g* for 3 min at 4°C in the dark. The supernatant from both aortic and plasma preparations was subjected to oxidation in acidic (0.2 M trichloroacetic acid with 2.5% I2 and 10% KI) and alkalytic solutions (0.1 M NaOH with 0.9% I2 and 1.5% KI). After centrifugation, 10 μl of the supernatant was injected into a HPLC system equipped with a fluorescent detector (Schimadzu America Inc, Carlsbad, CA, USA). Excitation and emission wavelengths of 350 nm and 450 nm were used to detect H_4B and its oxidized species. H_4B concentration was calculated according to a standard curve as we previously described [18,20,22,26].

2.12. Determination of DHFR activity using HPLC

DHFR activity was determined from isolated ECs or denuded aortic ring lysates as we previously described [19–22,26,29]. Briefly, lysates were incubated in a DHFR assay buffer (0.1 mol/L potassium phosphate

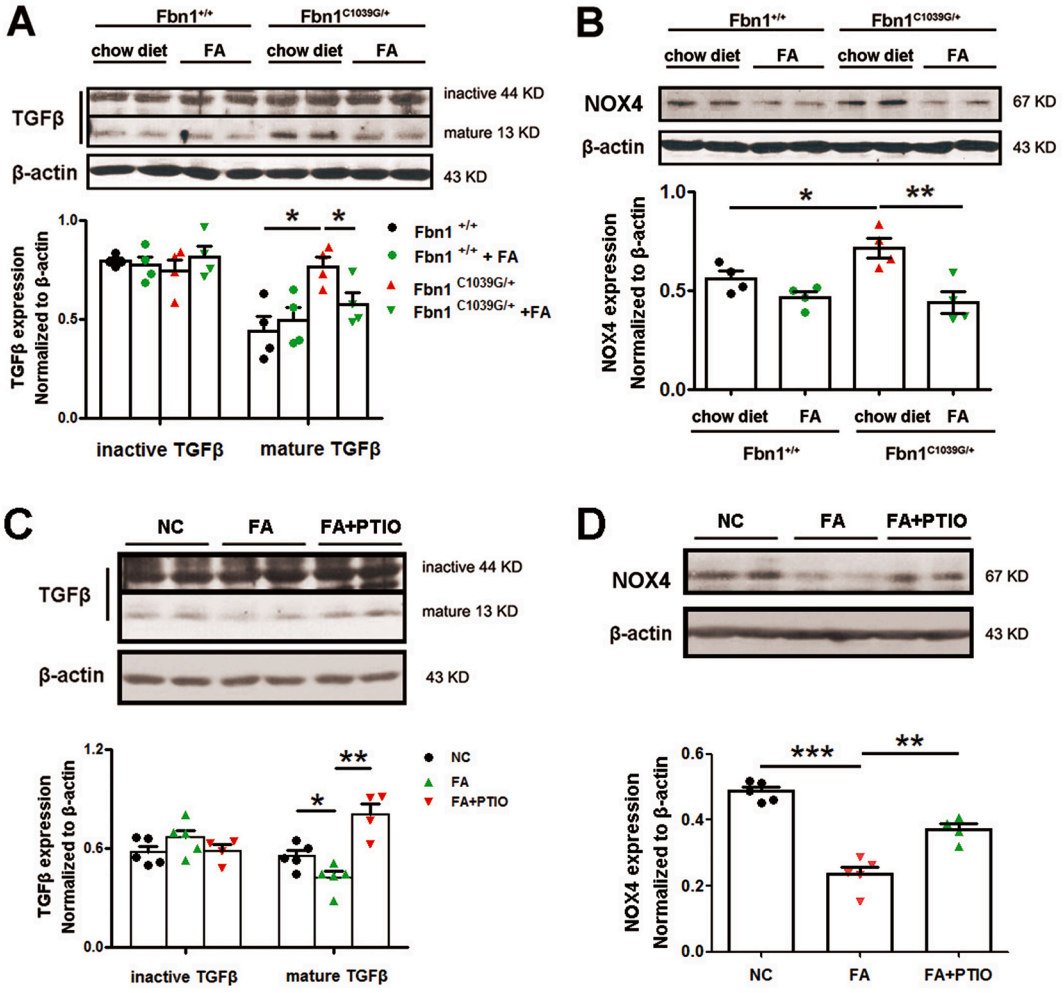

Fig. 8. Folic acid diet attenuates TGFβ and NOX4 expression in aortas of *Fbn1*$^{C1039G/+}$ mice and HAECs. *Fbn1*$^{+/+}$ and *Fbn1*$^{C1039G/+}$ mice of 4 weeks age were treated with FA diet (15 mg/kg/day) for 8 weeks, after which Western blotting was used to examine TGFβ and NOX4 expression levels in aortas. **(A)** Representative Western blots and grouped densitometric data of aortic protein expression levels of inactive and mature TGFβ, indicating downregulation of mature TGFβ after FA diet in *Fbn1*$^{C1039G/+}$ mice. Data are presented as Mean ± SEM, n = 4. **(B)** Representative Western blots and grouped densitometric data of aortic levels of NOX4 protein, indicating downregulation of NOX4 after FA diet in *Fbn1*$^{C1039G/+}$ mice. Data are presented as Mean ± SEM, n = 4. Human aortic endothelial cells (HAECs) were pretreated with 60 μmol/L PTIO for 1 h before FA treatment for 24 h, prior to examination of TGFβ and NOX4 protein expression by Western blotting analysis. **(C)** Representative Western blots and grouped densitometric data of inactive and mature TGFβ protein, indicating downregulation of mature TGFβ by FA and reversal by PTIO. **(D)** Representative Western blots and grouped densitometric data of NOX4 protein, indicating downregulation of NOX4 by FA and reversal by PTIO. Data are presented as Mean ± SEM, n = 4–5. *p < 0.05, **p < 0.01, ***p < 0.001.

dibasic, 1 mmol/L DTT, 0.5 mmol/L KCl, 1 mmol/L EDTA, and 20 mmol/L sodium ascorbate at pH 7.4) containing NADPH (200 μmol//L) and the substrate dihydrofolate (50 μmol/L) at 37°C for 20 min in the dark. The product of the reaction, tetrahydrofolate (THF), was measured using a HPLC system (Shimadzu America Inc., Carlsbad, CA, USA) with a C-18 column (Alltech, Deerfield, MA, USA) using water based mobile phase consisting of 7% acetonitrile and 5 mmol/L of potassium phosphate dibasic at pH 2.3. The signal was detected using a fluorescent detector at 295 nm excitation and 365 nm emission. The THF content was calculated against a standard curve prepared using THF solutions in assay buffer. Data are presented as nmol production of THF per min per mg protein.

2.13. *In vitro treatment with folic acid and PTIO*

Human aortic endothelial cells (HAECs, LONZA, as described above) were pretreated with NO scavenger 2-phenyl-4,4,5,5-tetramethylimidazoline-1-oxyl-3-oxide (PTIO, 60 μmol/L) as previously described [30,34,35] 1 h before folic acid (50 μmol/L) treatment [29] for 24 h. The protein expression levels of TGFβ and NOX4 were subsequently determined using Western blotting analyses.

2.14. *RNA interference with fibrillin 1 siRNA in the presence of anti-TGFβ*

Human fibrillin 1 siRNA (siRNA ID: s502520) and negative control siRNA were purchased from ThermoFisher Scientific (Waltham, MA, USA). HAECs were grown in 6-well plates until 70–80% confluence. Then, siRNA transfection was performed using Lipofectamine 2000 reagent (Thermo Fisher Invitrogen, USA) following manufacturer's instructions. After 24 h, anti-TGFβ (clone 1D11, Bio X Cell) or IgG (clone MOPC21, Bio X Cell) was added to the media and incubated for another 24 h. The cells were then harvested for Western blotting determination of GTPCHI protein expression.

2.15. *Statistical analysis*

All statistical analyses were performed using the Graphpad Prism software. All of the original data have been checked and found to distribute normally. Comparison between two groups was performed

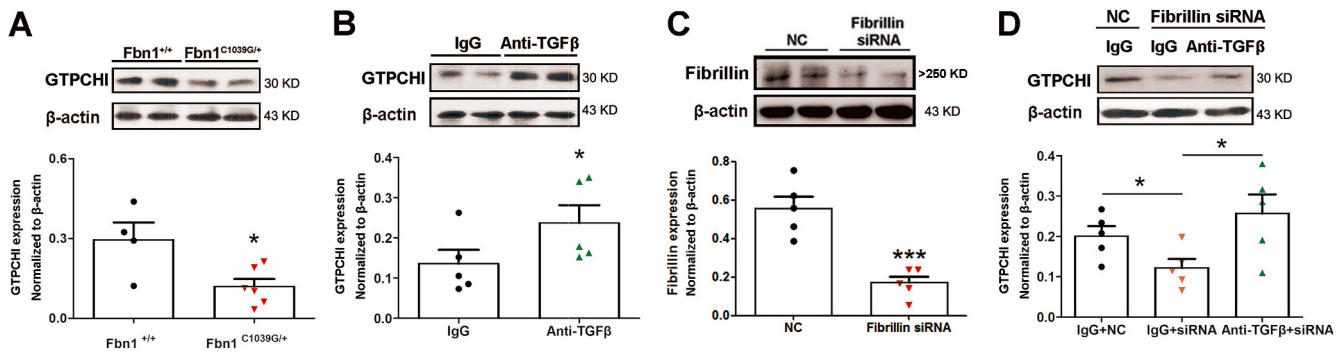

Fig. 9. TGFβ-dependent GTPCHI downregulation contributes to baseline deficiencies of H_4B and eNOS uncoupling in *Fbn1*$^{C1039G/+}$ animals. The aortas were isolated from 12 weeks old *Fbn1*$^{+/+}$ and *Fbn1*$^{C1039G/+}$ and subjected to Western blotting analysis to examine GTPCHI expression. **(A)** Representative Western blots and grouped densitometric data of aortic GTPCHI expression, indicating downregulation of GTPCHI in *Fbn1*$^{C1039G/+}$ mice. Data are presented as Mean ± SEM, n = 4–6. In parallel experiments, human aortic endothelial cells (HAECs) were treated by TGFβ blocking antibody with or without fibrillin siRNA transfection, after which cells were lysed for determination of GTPCHI protein expression by Western blotting. **(B)** Representative Western blots and grouped densitometric data of GTPCHI protein expression, indicating restoration of GTPCHI protein abundance with TGFβ blocking antibody. Data are presented as Mean ± SEM, n = 5. **(C)** Representative Western blots and grouped densitometric data of Fibrillin expression, confirming efficacy in silencing fibrillin expression with fibrillin siRNA. Data are presented as Mean ± SEM, n = 5. **(D)** Representative Western blots and grouped densitometric data of GTPCHI protein expression, indicating downregulation of GTPCHI by fibrillin deficiency, which was reversed by TGFβ blocking antibody. Data are presented as Mean ± SEM, n = 5. *p < 0.05, ***p < 0.001.

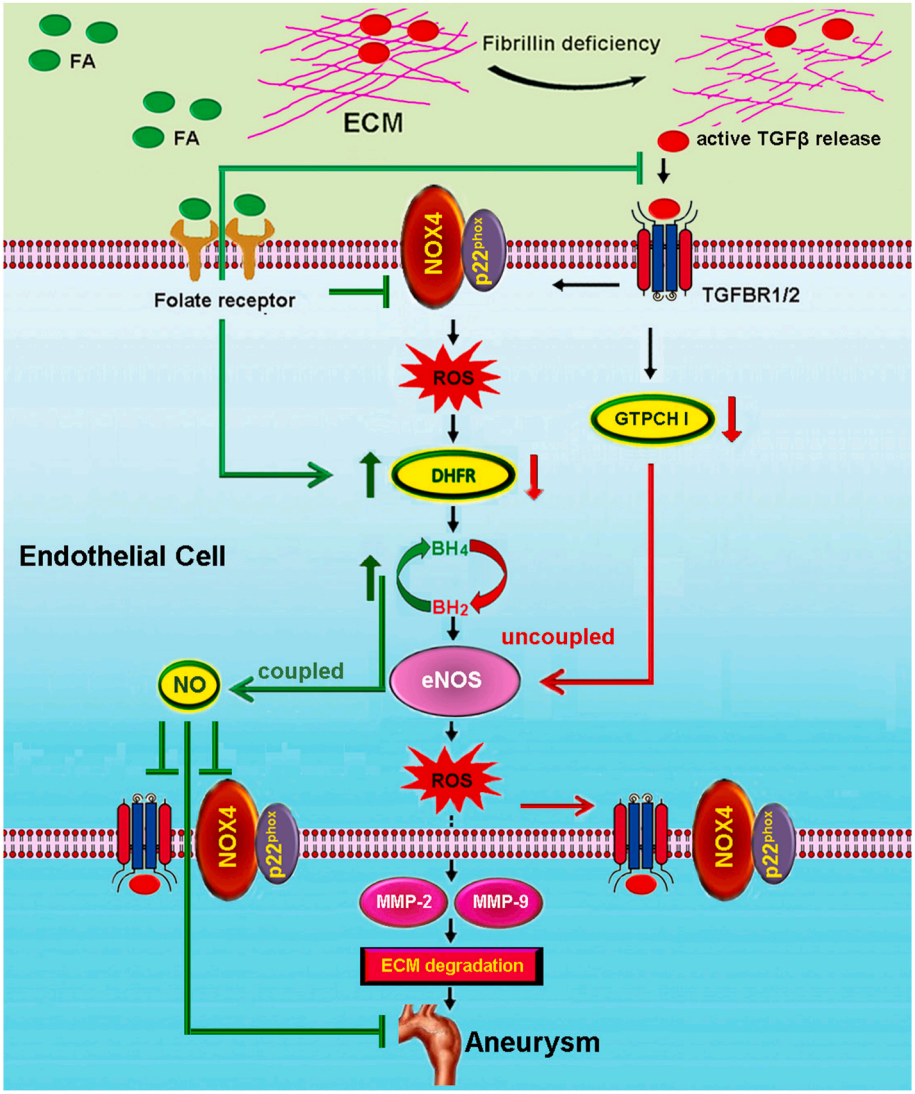

Fig. 10. Targeting feed-forward signaling of TGFβ/NOX4/DHFR/eNOS uncoupling/TGFβ axis with anti-TGFβ and folic acid attenuates formation of aortic aneurysms. Our data for the first time establish a novel feed-forward mechanism of TGFβ/NOX4/DHFR/eNOS uncoupling/TGFβ axis in the development of TAA in MFS mice, targeting of which with anti-TGFβ or FA diet (via DHFR/H_4B/eNOS recoupling/NO pathway) abrogates aneurysm formation in MFS mice. Notably, FA diet downregulated TGFβ and NOX4 protein expression, further disrupting the feed-forward loop to attenuate aneurysm formation. Correction of fibrillin is additionally beneficial in preserving GTPCHI protein abundance to maintain eNOS coupling activity.

using the student's t-test. Comparison among multiple groups was performed using ANOVA, followed by Newman-Keuls post-hoc test. Statistical significance was set at $p < 0.05$. All grouped data are presented as Mean ± SEM.

3. Results

Anti-TGFβ attenuates aneurysm formation in *Fbn1*$^{C1039G/+}$ animals via NOX4 inhibition, DHFR restoration, and recoupling of eNOS: Since the function of TGFβ signaling is controversial in TAA formation, we first examined protein expression of TGFβ and its downstream effector NOX4 in *Fbn1*$^{C1039G/+}$ mice. As shown in Fig. 1A, protein expression of mature TGFβ, rather than that of the inactive form of TGFβ, was upregulated by two fold in 12 weeks old *Fbn1*$^{C1039G/+}$ mice. The expression of NOX4 followed the same trend (Fig. 1B). Of note, the specificity of the NOX4 antibody was verified using NOX4 knockout mice (Supplemental Fig. 2), which were generous gifts of Dr. Junichi Sadoshima at the Rutgers University [36]. Our previous studies have shown that genetic deletion of NOX4 preserves DHFR protein abundance in the endothelium, resulting in recoupling of eNOS and attenuated AAA formation [21]. Similar to the AAA animals, endothelial specific DHFR expression was downregulated in *Fbn1*$^{C1039G/+}$ mice (Fig. 1C) by ~40%, which is attributed to TGFβ/NOX4 activation (see below on anti-TGFβ restoration of DHFR protein abundance). IHC staining was used to further examine DHFR protein expression in situ in 12 weeks old *Fbn1*$^{C1039G/+}$ mice. Of note, the expression of DHFR in the endothelial layer was markedly decreased in *Fbn1*$^{C1039G/+}$ mice compared to *Fbn1*$^{+/+}$ mice (Fig. 1D), which is consistent with Western blotting results in Fig. 1C.

In order to examine the potential upstream role of TGFβ in NOX4 activation, DHFR deficiency and eNOS uncoupling, *Fbn1*$^{C1039G/+}$ animals were treated with anti-TGFβ antibody in vivo. Of note, anti-TGFβ antibody significantly alleviated NOX4 protein upregulation (Fig. 1E), restored DHFR protein expression (Fig. 1F) and attenuated total ROS production (Fig. 1G) and eNOS uncoupling activity (Fig. 1H) in *Fbn1*$^{C1039G/+}$ mice. These data indicate that TGFβ lies upstream of NOX4 activation, and consequent DHFR deficiency and eNOS uncoupling.

Furthermore, we explored whether anti-TGFβ can prevent the expansion of aortic root and abdominal aorta in *Fbn1*$^{C1039G/+}$ mice. Ultrasound imaging was used to follow expansion of aortic roots and abdominal aortas in *Fbn1*$^{C1039G/+}$ mice from 4 weeks old, which had been treated with IgG or anti-TGFβ for 4 weeks. The aortic root diameter was reduced after treatment with anti-TGFβ antibody for 3 or 4 weeks in *Fbn1*$^{C1039G/+}$ mice (Fig. 2A and B), while there was yet significant difference in abdominal aorta diameter between anti-TGFβ and IgG treated group (Fig. 2C and D). We believe the latter is likely related to the relatively slower progression of AAA in *Fbn1*$^{C1039G/+}$ mice.

Recoupling of eNOS with oral administration of folic acid attenuates expansion of aortic root and abdominal aorta in *Fbn1*$^{C1039G/+}$ mice: We have previously shown that oral administration of FA attenuates AAA formation via recoupling eNOS in both novel and classical models of AAA including Ang II infused hph-1 mice and Ang II infused apoE null mice [18,19]. Here, we explored whether FA diet can prevent the expansion of aortic root and abdominal aorta in *Fbn1*$^{C1039G/+}$ mice. Ultrasound imaging was used to examine sizes of aortic roots and abdominal aortas in *Fbn1*$^{+/+}$ or *Fbn1*$^{C1039G/+}$ mice from 4 weeks old with or without FA treatment for 8 weeks. Of note, *Fbn1*$^{C1039G/+}$ mice displayed significant, time-dependent expansion of both aortic roots (Fig. 3A & B) and abdominal aortas (Fig. 4A & B) compared to the *Fbn1*$^{+/+}$, which was however near completely attenuated by treatment with FA diet (Fig. 3A–B; 4A-4B). Furthermore, histological evaluation by H&E staining indicated significant dilation of aortic roots (Fig. 3C) and abdominal aortas (Fig. 4C) in 12 weeks old *Fbn1*$^{C1039G/+}$ mice compared to 12 weeks old *Fbn1*$^{+/+}$ mice, which was completely abrogated by FA diet (Figs. 3C & 4C). Flattening and breakdown of elastic fibers of aortic roots (Fig. 3D) and abdominal aortas (Fig. 4D) were found in 12 weeks old *Fbn1*$^{C1039G/+}$ mice compared to age-matched *Fbn1*$^{+/+}$ mice as detected by Verhoeff-Van Gieson (VVG) staining. These disruptions in elastin fibers were abolished in animals fed FA diet (Figs. 3D & 4D). These results implicate that oral FA administration may serve as a robust treatment to attenuate aneurysm formation in MFS mice.

Folic acid diet reduces superoxide production, restores NO bioavailability and recouples eNOS in *Fbn1*$^{C1039G/+}$ mice: Consistent to the findings above that FA diet abolished aneurysm formation in *Fbn1*$^{C1039G/+}$ mice, and its remarkable effects in attenuating AAA formation in various novel and classical mouse models [18,19], FA diet completely alleviated superoxide production in *Fbn1*$^{C1039G/+}$ mice (Fig. 5A), which was accompanied by restored NO bioavailability in 8 weeks old and 12 weeks old mice (Fig. 5B) and attenuated eNOS uncoupling activity (Fig. 5C). Aortic superoxide production determined by ESR was significantly elevated in *Fbn1*$^{C1039G/+}$ mice at the age of 4, 8 and 12 weeks old compared to *Fbn1*$^{+/+}$ mice at the same age, which was completely attenuated by FA diet (started at four weeks of age and lasted for 4 and 8 weeks) (Fig. 5A). We next determined NO bioavailability in freshly isolated aortic segments from *Fbn1*$^{+/+}$ and *Fbn1*$^{C1039G/+}$ mice with or without oral FA administration. The results, shown in Fig. 5B, indicate that NO bioavailability was markedly diminished in the aortas of *Fbn1*$^{C1039G/+}$ mice comparing to the *Fbn1*$^{+/+}$ mice at 8 and 12 weeks old, while FA diet restored NO bioavailability (Fig. 5B).

Oral FA administration is anticipated to recouple eNOS in vivo as we previously shown [18,19,29]. If eNOS is functional and coupled, its inhibition by L-NAME will increase the measured superoxide due to lack of scavenging effects of NO on superoxide. However, if eNOS is dysfunctional and uncoupled, it produces superoxide and the inhibition with L-NAME will reduce measured superoxide. Hence, the difference between the superoxide values measured with and without L-NAME reflects the coupling/uncoupling status of eNOS. As is obvious in Fig. 5C, L-NAME-sensitive superoxide production, reflective of eNOS uncoupling activity, was significantly increased in *Fbn1*$^{C1039G/+}$ mice at 4, 8 and 12 week old, which was completely attenuated by FA diet. These results indicate that FA prevented aneurysm formation via recoupling of eNOS to shut down eNOS-derived superoxide production, sustained oxidative stress, and consequent matrix degradation, similar to what we have shown for AAA formation.

Folic acid diet restores tissue and circulating H_4B levels in *Fbn1*$^{C1039G/+}$ animals, and a biomarker role of circulating H_4B for TAA: We and others have shown that uncoupling of eNOS is caused by a deficiency in H_4B [16,17]. Therefore, aortic and plasma H_4B bioavailability was determined by HPLC in *Fbn1*$^{+/+}$ and *Fbn1*$^{C1039G/+}$ animals at 4, 8 and 12 weeks old. The results in Fig. 6A & 6B indicate that aortic and circulating H_4B levels in *Fbn1*$^{C1039G/+}$ mice were significantly reduced compared to that of *Fbn1*$^{+/+}$ mice starting from 4 weeks old, but fully restored with FA diet. We have previously shown that circulating H_4B serves as a novel biomarker for AAA [37]. As shown in Fig. 6B, changes in circulating levels of H_4B aligned well with that of tissue levels (Fig. 6A); and FA diet was able to restore both tissue and circulating H_4B levels. Linear correlation between aortic and plasma H_4B levels was calculated. As shown in Fig. 6C, circulating H_4B levels accurately predicted tissue H_4B levels. The reduced H_4B levels also correlated well with increased aortic root diameters in *Fbn1*$^{C1039G/+}$ animals (Fig. 6D & 6E). Besides, reduced H_4B levels correlated well with increased abdominal aorta diameters in *Fbn1*$^{C1039G/+}$ animals (Fig. 6F & 6G). These results indicate that H_4B deficiency is involved in eNOS uncoupling-dependent aneurysm formation, which was reversed by oral FA administration. In addition, circulating H_4B levels may be used clinically as a novel biomarker for the development and treatment response of TAA and AAA, which is quantitatively predictive of aneurysm sizes.

Folic acid diet upregulates endothelial DHFR protein expression and activity in *Fbn1*$^{C1039/+}$ mice: Data described above indicate that restoration of eNOS coupling activity following improved H_4B

bioavailability mediates the protective effects of FA diet on TAA formation. Our previous studies have shown that oral FA administration recouples eNOS through augmentation of endothelial DHFR expression and activity [18,19,29]. Here, we examined endothelial DHFR expression and activity in *Fbn1*$^{C1039G/+}$ mice in response to oral FA administration. Endothelial cells (ECs) were isolated from freshly prepared aortas. As shown by the representative Western blots and grouped data (Fig. 7A-7B), endothelial specific expression of DHFR was significantly upregulated in both *Fbn1*$^{+/+}$ and *Fbn1*$^{C1039G/+}$ animals after FA treatment, while eNOS protein expression was downregulated (Fig. 7C). Furthermore, IHC staining confirmed upregulated DHFR expression in *Fbn1*$^{C1039G/+}$ mice fed FA diet (Fig. 7D). It should be pointed out that eNOS protein upregulation when uncoupled is a deteriorating response. Previous studies have shown that eNOS expression was upregulated in Ang II infused hph-1 mice and apoE null mice at baseline when eNOS is uncoupled [18,38]. Similar trend has also been observed in apoE null mice and DOCA-salt hypertensive mice [38,39]. As shown in Fig. 7E & 7F, DHFR activity in the isolated ECs and the denuded aortas of *Fbn1*$^{C1039G/+}$ mice were both increased by oral FA administration. Taken together, these data indicate that FA recoupling of eNOS to attenuate TAA formation was attributed to improvement in DHFR expression and activity in *Fbn1*$^{C1039G/+}$ mice.

Folic acid diet attenuates NOX4 and TGFβ expression in aortas of *Fbn1*$^{C1039G/+}$ mice: To examine whether there is a feed-forward activation of uncoupled eNOS on TGFβ/NOX4 that can be interrupted by FA diet, we examined aortic TGFβ and NOX4 protein expression in FA diet fed *Fbn1*$^{C1039G/+}$ mice and wild type controls. The protein expression of TGFβ (Fig. 8A) and NOX4 (Fig. 8B) were significantly decreased in *Fbn1*$^{C1039G/+}$ animals after oral FA administration. Therefore, there seems to be a feed-forward activation of eNOS uncoupling on TGFβ and NOX4, which would further sustain the TGFβ/NOX4/DHFR/eNOS uncoupling pathway to lead to prolonged oxidative stress and aneurysm formation. Since p22phox is the catalytic regulatory subunit of NOX4 and other NOX isoforms on the membrane [17], we also examined expression of p22phox in *Fbn1*$^{C1039G/+}$ mice. The expression of p22phox was not altered in *Fbn1*$^{C1039G/+}$ mice compare to *Fbn1*$^{+/+}$ mice; or by oral FA administration (Supplemental Fig. 3).

In additional experiments, HAECs were pretreated with 60 μmol/L PTIO 1 h before FA treatment to examine whether FA regulation of TGFβ and NOX4 is NO-dependent, conseqent to folic acid recoupling of eNOS. The results revealed that FA attenuation of mature TGFβ and NOX4 expression was reversed by PTIO (Fig. 8C & D), indicating a NO dependency.

TGFβ-dependent GTPCHI downregulation contributes to baseline deficiencies of H_4B and eNOS uncoupling in *Fbn1*$^{C1039G/+}$ animals: Since there is a baseline deficiency in H_4B in 4 weeks old *Fbn1*$^{C1039G/+}$ mice while DHFR only became deficient at 8 weeks old, we examined a potential baseline deficiency in the rate limiting H_4B synthetic enzyme GTPCHI. The results indicate that GTPCHI protein abundance was significantly lower in *Fbn1*$^{C1039G/+}$ mice comparing to the wild type mice (Fig. 9A). This response likely underlies reduced H_4B bioavailability at baseline, whereas the beneficial effects of FA on improving H_4B bioavailability to recouple eNOS is mediated by upregulation in DHFR expression and activity.

In order to examine a potential role of TGFβ in regulating GTPCHI expression in the presence of fibrillin deficiency, HAECs were treated with anti-TGFβ antibody in the presence or absence of fibrillin siRNA. The anti-TGFβ antibody treatment alone significantly upregulated GTPCHI protein abundance in HAECs (Fig. 9B). Furthermore, while fibrillin siRNA (significantly decreased Fibrillin protein expression, Fig. 9C) induced significant reduction in GTPCHI protein expression (Fig. 9D) that is similar with what we observed in vivo in Fbn1 mice (Fig. 9A), anti-TGFβ treatment preserved GTPCHI protein abundance under fibrillin siRNA transfection (Fig. 9D), indicating TGFβ-dependent downregulation of GTPCHI protein expression in the presence of fibrillin deficiency. Therefore, the deficiencies in H_4B and eNOS coupling activity at baseline seem attributed to TGFβ-dependent downregulation of GTPCHI in *Fbn1*$^{C1039G/+}$ mice.

Taken together, our findings in the present study reveal a novel, feed-forward TGFβ/NOX4/DHFR/eNOS uncoupling/TGFβ signaling axis in mediating TAA formation in *Fbn1*$^{C1039G/+}$ mice. Antagonism of TGFβ signaling with anti-TGFβ in vivo or recoupling of eNOS with FA diet substantially attenuated aneurysm formation. FA further decreased NOX4 and TGFβ expression to shut down the feed-forward mechanism. Correction of fibrillin deficiency is additionally beneficial in preserving GTPCHI function to maintain eNOS coupling activity at baseline. These data elucidate novel mechanisms and therapeutics for TAA formation, which are highly translational in promoting development of anti-TGFβ and FA-based oral medicines for the treatment of aortic aneurysms.

4. Discussion

The most significant findings of the present study are the first demonstration of a novel feed-forward pathway of TGFβ/NOX4/DHFR/eNOS uncoupling/TGFβ in TAA and AAA formation in Marfan mice, and the robust therapeutic potential for aortic aneurysm of TGFβ antagonism and eNOS recoupling by anti-TGFβ and FA diet in vivo (Fig. 10). The expression of mature/active TGFβ and its downstream effector NOX4 were upregulated while DHFR was downregulated in *Fbn1*$^{C1039G/+}$ mice. In vivo administration with anti-TGFβ attenuated aneurysm formation via inactivation of NOX4/DHFR deficiency/eNOS uncoupling pathway. Intriguingly, oral administration of FA attenuates echo defined expansion of aortic roots and abdominal aortas via restoration of endothelial DHFR function and H_4B bioavailability, which recouples eNOS and restores NO bioavailability in *Fbn1*$^{C1039G/+}$ mice. Circulating levels of H_4B are accurately reflective of aortic H_4B levels, and that aortic and circulating H_4B levels are negatively correlated with diameters of aortic roots and abdominal aorta, indicating a novel biomarker role of circulating H_4B for TAA and AAA. FA diet also attenuated TGFβ and NOX4 expression to further inactivate the feed-forward mechanism of the TGFβ/NOX4/DHFR/eNOS uncoupling axis to abrogate aneurysm formation in *Fbn1*$^{C1039G/+}$ mice.

The role of TGFβ signaling in TAA formation in different animal models is different or controversial [8–10]. *Fbn1*$^{C1039G/+}$ and *Fbn1*$^{mgR/mgR}$ mice have been used to explore the function of TGFβ and its downstream pathways in TAA formation [12,15,40]. MFS mice with non-dissecting TAA (*Fbn1*$^{C1039G/+}$ mice) developed aneurysm as a result of overly produced TGFβ to activate phosphorylation and subsequent nuclear translocation of Smad2, which leads to disruption of elastic fiber [11]. Besides, noncanonical (smad-independent) TGFβ signaling was shown to drive aortic aneurysm formation in *Fbn1*$^{C1039G/+}$ mice [12]. Long-term treatment with doxycycline suppressed TGFβ upregulation, while inhibiting MMP-2 and MMP-9 activation to attenuate TAA formation in *Fbn1*$^{C1039G/+}$ mice [41]. On the other hand, in a more severe model (*Fbn1*$^{mgR/mgR}$ mice), anti-TGFβ either exacerbated or attenuated TAA formation depending on whether treatment was initiated before (postnatal day 16; P16) or after (P45) aneurysm formation, respectively [15]. Xiong et al. found that doxycycline delays the manifestations of MFS, in part, through its ability to decrease active TGFβ and the noncanonical signaling cascade downstream of TGFβ in *Fbn1*$^{mgR/mgR}$ mice [40]. In Ang II infused C57BL/6J mice, aortic rupture and aneurysm in both thoracic and abdominal regions is enhanced by TGFβ neutralization when initiated before pathogenesis [42]. In the present study, we identified a clear causal role of TGFβ signaling in activating a feedforward mechanism of NOX4/DHFR/eNOS uncoupling to result in aneurysm formation in *Fbn1*$^{C1039G/+}$ mice. The upstream role of TGFβ is consistent with previous findings in this particular model of Marfan aneurysms [12]. Notably, we also found that FA is an effective therapeutic when initiated both before (AAA yet formed in 4 weeks old *Fbn1*$^{C1039G/+}$ mice) and after (TAA already started in 4 weeks old *Fbn1*$^{C1039G/+}$ mice) aneurysm formation. Besides, anti-TGFβ also proved to be an effective therapeutic to attenuate aneurysm progression started

in 4 weeks old *Fbn1*$^{C1039G/+}$ mice.

NOX4 has been shown to lie downstream of TGFβ in aneurysm formation and progression in *Fbn1*$^{C1039G/+}$ mice [14]. Knockout of NOX4 resulted in abrogated aortic root expansion in *Fbn1*$^{C1039G/+}$ mice [14]. In the present study we observed NOX4 upregulation in *Fbn1*$^{C1039G/+}$ mice, inhibition of which with anti-TGFβ attenuated eNOS uncoupling and aneurysm formation, indicating a novel upstream role of TGFβ/NOX4 in driving eNOS uncoupling-dependent aneurysm formation. Of note, the expression of p22phox was not changed in *Fbn1*$^{C1039G/+}$ mice compared to *Fbn1*$^{+/+}$ mice, indicating that TGFβ modulation of NOX4 activity in *Fbn1*$^{C1039G/+}$ mice was independent of any regulation in p22phox. Interestingly, using hph-1/NOX1, hph-1/NOX2 and hph-1/NOX4 double mutant mice, we have previously demonstrated roles of NOX isoforms in AAA formation in Ang II infused animals [21]. Among the three NOX isoforms, deletion of NOX4 in hph-1 mice is most robust in attenuating AAA formation. Furthermore, we have identified two novel mutations in human patients with AAA, which are associated with significant elevation in ROS production [21]. Taken together, these data demonstrate that NOX4 plays a critical role in the formation of aortic aneurysms including TAA and AAA under Marfan syndrome condition, or not.

The role of NOX4 in aneurysm formation is mediated by eNOS uncoupling. Activation of NOX leads to eNOS uncoupling and activation of other secondary oxidase systems [16,17]. We have previously shown that NOX activation-dependent deficiency in DHFR induces eNOS uncoupling in cultured endothelial cells, and in animals with hypertension, aortic aneurysms, diabetic vascular dysfunction and cardiac I/R injury [18,19,21,22,26–29,31,43]. We also clarified that NOX4 is the most effective target when inhibited, in attenuating AAA formation in hph-1 mice via recoupling eNOS [21]. Here, we observed upregulated NOX4 and eNOS uncoupling in *Fbn1*$^{C1039G/+}$ mice, while anti-TGFβ successful recoupled eNOS via downregulation of NOX4. These findings indicate that NOX4/eNOS uncoupling axis lies downstream of TGFβ activation to mediate TAA formation in *Fbn1*$^{C1039G/+}$ mice.

We have previously established a novel and important role of eNOS uncoupling in AAA formation, and demonstrated robust efficacy of oral FA administration in attenuating AAA formation in Ang II-infused hph-1 and apoE null mice [18,19]. Here we examined whether oxidative stress and uncoupled eNOS are responsible for TAA formation in *Fbn1*$^{C1039G/+}$ mice, and made a thorough inquiry if FA diet could be used as a potential oral medicine for TAA treatment. A correlation between oxidative stress and severity of TAA was previously documented [44]. Excessive production of ROS has been implicated as a pathogenetic mechanism in aortic aneurysm formation and other manifestations occurring in MFS [44,45]. In the present study we observed that eNOS was uncoupled in *Fbn1*$^{C1039G/+}$ mice to produce superoxide, and our data represent the first evidence that eNOS uncoupling serves as a primary source of ROS for TAA formation. Oral administration with FA is highly effective in recoupling eNOS to attenuate TAA and AAA formation in *Fbn1*$^{C1039G/+}$ mice. Our results show that FA completely restores eNOS coupling activity to improve NO bioavailability, resulting in abrogated expansion of aortic roots and abdominal aortas in *Fbn1*$^{C1039G/+}$ mice. These data demonstrate that FA diet could represent a novel therapeutic strategy for aneurysm formation in *Fbn1*$^{C1039G/+}$ mice, which may be broadly useful to treat TAA of alternative causes as well. Besides oxidative stress, hypertension is considered a risk factor and mechanism for aortic aneurysms [46]. Uncoupling of eNOS has been shown to occur in spontaneously hypertensive rats (SHRs) [47], stroke-prone SHRs [48], Ang II induced hypertension [18] and hypertension induced with the DOCA [39,49]. We have previously demonstrated that FA treatment normalizes blood pressure in Ang II infused mice via restoration of eNOS coupling activity [18]. Therefore, we believe that FA has the potential to also particularly attenuate TAA formation in patients with co-existing hypertension.

Others and we have shown that H_4B deficiency switches eNOS from the coupled to the uncoupled state [16–18,27–29,50–52]. In the present study we found that aortic and circulating H_4B levels were significantly reduced in *Fbn1*$^{C1039G/+}$ mice, which was accompanied by eNOS uncoupling activity. Our results further indicate that oral administration of FA restored H_4B bioavailability in both aortic tissues and plasma, which was associated with abrogated eNOS uncoupling activity and attenuation of TAA formation in *Fbn1*$^{C1039G/+}$ mice. Of note, aortic and plasma H_4B levels were quantitatively correlated with sizes of aortic roots and abdominal aorta, with lower H_4B levels corresponding to bigger aortic root and abdominal aortic dimensions. Therefore, our data for the first time demonstrate a novel biomarker role of circulating H_4B for the formation of TAA and AAA that is quantitatively predictive of aneurysm sizes, which may be used clinically for monitoring of the disease progression and response to treatments.

We have previously shown that endothelial DHFR deficiency induces a reduction in H_4B bioavailability and consequent eNOS uncoupling to result in development of cardiovascular diseases, including hypertension, aortic aneurysms, and diabetic vascular complications [18–22,26,29,31]. The endothelial expression and activity of DHFR were significantly upregulated in FA diet treated *Fbn1*$^{C1039G/+}$ mice, indicating a novel observation of DHFR-dependent attenuation of aneurysm formation. This is consistent to our previous findings in AAA where FA diet restoration of DHFR function is preventive of AAA formation [18,19,21]. It's worth noting that there was a reduction in GTPCHI protein expression that seems to account for H_4B deficiency in *Fbn1*$^{C1039G/+}$ animals at baseline. Furthermore, our in vitro study in HAECs demonstrated that GTPCHI is downstream of TGFβ in the presence of Fbn1 deficiency. Importantly, we also found that the expression of TGFβ and NOX4 were significantly attenuated by FA diet in *Fbn1*$^{C1039G/+}$ animals, indicating efficacy of FA in disrupting the feed-forward loop of eNOS uncoupling-TGFβ to shut down the pathway responsible for aneurysm formation. Of note, this inhibitory effect of FA on TGFβ and NOX4 was found dependent on an intermediate role of NO that is produced from recoupled eNOS in response to FA treatment.

In summary, our data for the first time reveal a novel, feed-forward mechanism of TGFβ/NOX4/DHFR/eNOS uncoupling/TGFβ signaling in mediating aneurysm formation in MFS mice. Targeting this pathway with anti-TGFβ or oral FA administration is robustly effective in attenuating both TAA and AAA formation. By recoupling eNOS to produce NO, FA further downregulates TGFβ/NOX4 expression to disrupt the feed-forward loop. Correction of fibrillin deficiency is additionally beneficial in preserving GTPCHI function to maintain eNOS coupling activity at baseline. These data reveal novel mechanisms and therapeutics for aneurysm formation, which are highly translational in promoting development of anti-TGFβ and FA-based oral medicines for the treatment of aortic aneurysms.

Funding

This study was supported by National Institute of Health National Heart, Lung and Blood Institute (NHLBI) Grants HL077440 (HC), HL088975 (HC), HL119968 (HC), HL142951 (HC), HL154754 (HC) and an American Heart Association Established Investigator Award (EIA) 12EIA8990025 (HC).

Declaration of competing interest

None declared.

Appendix A. Supplementary data

Supplementary data to this article can be found online at https://doi.org/10.1016/j.redox.2020.101757.

References

[1] S.S. Virani, A. Alonso, E.J. Benjamin, M.S. Bittencourt, C.W. Callaway, A.P. Carson, A.M. Chamberlain, A.R. Chang, S. Cheng, F.N. Delling, L. Djousse, M.S.V. Elkind, J. F. Ferguson, M. Fornage, S.S. Khan, B.M. Kissela, K.L. Knutson, T.W. Kwan, D. T. Lackland, T.T. Lewis, J.H. Lichtman, C.T. Longenecker, M.S. Loop, P.L. Lutsey, S. S. Martin, K. Matsushita, A.E. Moran, M.E. Mussolino, A.M. Perak, W.D. Rosamond, G.A. Roth, U.K.A. Sampson, G.M. Satou, E.B. Schroeder, S.H. Shah, C.M. Shay, N. L. Spartano, A. Stokes, D.L. Tirschwell, L.B. VanWagner, C.W. Tsao, American Heart Association Council on E, Prevention Statistics C, Stroke Statistics S. Heart disease and stroke statistics-2020 update: a report from the american heart association, Circulation 141 (2020) e139–e596.

[2] E.M. Isselbacher, C.L. Lino Cardenas, M.E. Lindsay, Hereditary influence in thoracic aortic aneurysm and dissection, Circulation 133 (2016) 2516–2528.

[3] J.D. Humphrey, M.A. Schwartz, G. Tellides, D.M. Milewicz, Role of mechanotransduction in vascular biology: focus on thoracic aortic aneurysms and dissections, Circ. Res. 116 (2015) 1448–1461.

[4] K.E. Boczar, K. Cheung, M. Boodhwani, L. Beauchesne, C. Dennie, S. Nagpal, K. Chan, T. Coutinho, Sex differences in thoracic aortic aneurysm growth, Hypertension 73 (2019) 190–196.

[5] J. Raffort, F. Lareyre, M. Clement, R. Hassen-Khodja, G. Chinetti, Z. Mallat, Diabetes and aortic aneurysm: current state of the art, Cardiovasc. Res. 114 (2018) 1702–1713.

[6] S.C. Larsson, A.M. Mason, M. Back, D. Klarin, S.M. Damrauer, P. Million Veteran, K. Michaelsson, S. Burgess, Genetic predisposition to smoking in relation to 14 cardiovascular diseases, Eur. Heart J. 41 (2020) 3304–3310.

[7] M.J. Sherratt, T.J. Wess, C. Baldock, J. Ashworth, P.P. Purslow, C.A. Shuttleworth, C.M. Kielty, Fibrillin-rich microfibrils of the extracellular matrix: ultrastructure and assembly, Micron 32 (2001) 185–200.

[8] A. Daugherty, Z. Chen, H. Sawada, D.L. Rateri, M.B. Sheppard, Transforming growth factor-beta in thoracic aortic aneurysms: good, bad, or irrelevant? J Am Heart Assoc 6 (2017).

[9] J.B. Michel, G. Jondeau, D.M. Milewicz, From genetics to response to injury: vascular smooth muscle cells in aneurysms and dissections of the ascending aorta, Cardiovasc. Res. 114 (2018) 578–589.

[10] D.M. Milewicz, S.K. Prakash, F. Ramirez, Therapeutics targeting drivers of thoracic aortic aneurysms and acute aortic dissections: insights from predisposing genes and mouse models, Annu. Rev. Med. 68 (2017) 51–67.

[11] J.P. Habashi, D.P. Judge, T.M. Holm, R.D. Cohn, B.L. Loeys, T.K. Cooper, L. Myers, E.C. Klein, G. Liu, C. Calvi, M. Podowski, E.R. Neptune, M.K. Halushka, D. Bedja, K. Gabrielson, D.B. Rifkin, L. Carta, F. Ramirez, D.L. Huso, H.C. Dietz, Losartan, an at1 antagonist, prevents aortic aneurysm in a mouse model of marfan syndrome, Science 312 (2006) 117–121.

[12] T.M. Holm, J.P. Habashi, J.J. Doyle, D. Bedja, Y. Chen, C. van Erp, M.E. Lindsay, D. Kim, F. Schoenhoff, R.D. Cohn, B.L. Loeys, C.J. Thomas, S. Patnaik, J. J. Marugan, D.P. Judge, H.C. Dietz, Noncanonical tgfbeta signaling contributes to aortic aneurysm progression in marfan syndrome mice, Science 332 (2011) 358–361.

[13] Y. Onetti, T. Meirelles, A.P. Dantas, K. Schroder, E. Vila, G. Egea, F. Jimenez-Altayo, Nadph oxidase 4 attenuates cerebral artery changes during the progression of marfan syndrome, Am. J. Physiol. Heart Circ. Physiol. 310 (2016) H1081–H1090.

[14] F. Jimenez-Altayo, T. Meirelles, E. Crosas-Molist, M.A. Sorolla, D.G. Del Blanco, J. Lopez-Luque, A. Mas-Stachurska, A.M. Siegert, F. Bonorino, L. Barbera, C. Garcia, E. Condom, M. Sitges, F. Rodriguez-Pascual, F. Laurindo, K. Schroder, J. Ros, I. Fabregat, G. Egea, Redox stress in marfan syndrome: dissecting the role of the nadph oxidase nox4 in aortic aneurysm, Free Radic. Biol. Med. 118 (2018) 44–58.

[15] J.R. Cook, N.P. Clayton, L. Carta, J. Galatioto, E. Chiu, S. Smaldone, C.A. Nelson, S. H. Cheng, B.M. Wentworth, F. Ramirez, Dimorphic effects of transforming growth factor-beta signaling during aortic aneurysm progression in mice suggest a combinatorial therapy for marfan syndrome, Arterioscler. Thromb. Vasc. Biol. 35 (2015) 911–917.

[16] Q. Li, J.Y. Youn, H. Cai, Mechanisms and consequences of endothelial nitric oxide synthase dysfunction in hypertension, J. Hypertens. 33 (2015) 1128–1136.

[17] Y. Zhang, P. Murugesan, K. Huang, H. Cai, NADPH oxidases and oxidase crosstalk in cardiovascular diseases: novel therapeutic targets, Nat. Rev. Cardiol. 17 (2019) 170–194.

[18] L. Gao, K.L. Siu, K. Chalupsky, A. Nguyen, P. Chen, N.L. Weintraub, Z. Galis, H. Cai, Role of uncoupled endothelial nitric oxide synthase in abdominal aortic aneurysm formation: treatment with folic acid, Hypertension 59 (2012) 158–166.

[19] K.L. Siu, X.N. Miao, H. Cai, Recoupling of enos with folic acid prevents abdominal aortic aneurysm formation in angiotensin ii-infused apolipoprotein e null mice, PloS One 9 (2014), e88899.

[20] X.N. Miao, K.L. Siu, H. Cai, Nifedipine attenuation of abdominal aortic aneurysm in hypertensive and non-hypertensive mice: mechanisms and implications, J. Mol. Cell. Cardiol. 87 (2015) 152–159.

[21] K.L. Siu, Q. Li, Y. Zhang, J. Guo, J.Y. Youn, J. Du, H. Cai, Nox isoforms in the development of abdominal aortic aneurysm, Redox biology 11 (2017) 118–125.

[22] Q. Li, J.Y. Youn, K.L. Siu, P. Murugesan, Y. Zhang, H. Cai, Knockout of dihydrofolate reductase in mice induces hypertension and abdominal aortic aneurysm via mitochondrial dysfunction, Redox biology 24 (2019) 101185.

[23] C. Olsson, S. Thelin, E. Stahle, A. Ekbom, F. Granath, Thoracic aortic aneurysm and dissection: increasing prevalence and improved outcomes reported in a nationwide population-based study of more than 14,000 cases from 1987 to 2002, Circulation 114 (2006) 2611–2618.

[24] L.R. Bons, O.L. Rueda-Ochoa, K. El Ghoul, S. Rohde, R.P. Budde, M.J. Leening, M. W. Vernooij, O.H. Franco, A. van der Lugt, J.W. Roos-Hesselink, M. Kavousi, D. Bos, Sex-specific distributions and determinants of thoracic aortic diameters in the elderly, Heart 106 (2020) 133–139.

[25] L.S. Manlove, K.E. Berquam-Vrieze, K.E. Pauken, R.T. Williams, M.K. Jenkins, M. A. Farrar, Adaptive immunity to leukemia is inhibited by cross-reactive induced regulatory t cells, J. Immunol. 195 (2015) 4028–4037.

[26] H. Li, Q. Li, Y. Zhang, W. Liu, B. Gu, T. Narumi, K.L. Siu, J.Y. Youn, P. Liu, X. Yang, H. Cai, Novel treatment of hypertension by specifically targeting e2f for restoration of endothelial dihydrofolate reductase and enos function under oxidative stress, Hypertension 73 (2019) 179–189.

[27] K. Chalupsky, H. Cai, Endothelial dihydrofolate reductase: critical for nitric oxide bioavailability and role in angiotensin ii uncoupling of endothelial nitric oxide synthase, Proc. Natl. Acad. Sci. U.S.A. 102 (2005) 9056–9061.

[28] J.H. Oak, H. Cai, Attenuation of angiotensin ii signaling recouples enos and inhibits nonendothelial nox activity in diabetic mice, Diabetes 56 (2007) 118–126.

[29] L. Gao, K. Chalupsky, E. Stefani, H. Cai, Mechanistic insights into folic acid-dependent vascular protection: dihydrofolate reductase (dhfr)-mediated reduction in oxidant stress in endothelial cells and angiotensin ii-infused mice: a novel hplc-based fluorescent assay for dhfr activity, J. Mol. Cell. Cardiol. 47 (2009) 752–760.

[30] J. Zhang, H. Cai, Netrin-1 prevents ischemia/reperfusion-induced myocardial infarction via a dcc/erk1/2/enos s1177/no/dcc feed-forward mechanism, J. Mol. Cell. Cardiol. 48 (2010) 1060–1070.

[31] J.Y. Youn, L. Gao, H. Cai, The p47phox- and nadph oxidase organiser 1 (noxo1)-dependent activation of nadph oxidase 1 (nox1) mediates endothelial nitric oxide synthase (enos) uncoupling and endothelial dysfunction in a streptozotocin-induced murine model of diabetes, Diabetologia 55 (2012) 2069–2079.

[32] Q. Li, P. Wang, K. Ye, H. Cai, Central role of siah inhibition in dcc-dependent cardioprotection provoked by netrin-1/no, Proc. Natl. Acad. Sci. U.S.A. 112 (2015) 899–904.

[33] J.Y. Youn, J. Zhou, H. Cai, Bone morphogenic protein 4 mediates nox1-dependent enos uncoupling, endothelial dysfunction, and cox2 induction in type 2 diabetes mellitus, Mol. Endocrinol. 29 (2015) 1123–1133.

[34] A. Nguyen, H. Cai, Netrin-1 induces angiogenesis via a dcc-dependent erk1/2-enos feed-forward mechanism, Proc. Natl. Acad. Sci. U.S.A. 103 (2006) 6530–6535.

[35] N.M. Liu, K.L. Siu, J.Y. Youn, H. Cai, Attenuation of neointimal formation with netrin-1 and netrin-1 preconditioned endothelial progenitor cells, J. Mol. Med. 95 (2017) 335–348.

[36] S. Matsushima, J. Kuroda, T. Ago, P. Zhai, Y. Ikeda, S. Oka, G.H. Fong, R. Tian, J. Sadoshima, Broad suppression of nadph oxidase activity exacerbates ischemia/reperfusion injury through inadvertent downregulation of hypoxia-inducible factor-1alpha and upregulation of peroxisome proliferator-activated receptor-alpha, Circ. Res. 112 (2013) 1135–1149.

[37] K.L. Siu, H. Cai, Circulating tetrahydrobiopterin as a novel biomarker for abdominal aortic aneurysm, Am. J. Physiol. Heart Circ. Physiol. 307 (2014) H1559–H1564.

[38] J.B. Laursen, M. Somers, S. Kurz, L. McCann, A. Warnholtz, B.A. Freeman, M. Tarpey, T. Fukai, D.G. Harrison, Endothelial regulation of vasomotion in apoe-deficient mice: implications for interactions between peroxynitrite and tetrahydrobiopterin, Circulation 103 (2001) 1282–1288.

[39] J.Y. Youn, T. Wang, J. Blair, K.M. Laude, J.H. Oak, L.A. McCann, D.G. Harrison, H. Cai, Endothelium-specific sepiapterin reductase deficiency in doca-salt hypertension, Am. J. Physiol. Heart Circ. Physiol. 302 (2012) H2243–H2249.

[40] W. Xiong, T. Meisinger, R. Knispel, J.M. Worth, B.T. Baxter, Mmp-2 regulates erk1/2 phosphorylation and aortic dilatation in marfan syndrome, Circ. Res. 110 (2012) e92–e101.

[41] A.W. Chung, H.H. Yang, M.W. Radomski, C. van Breemen, Long-term doxycycline is more effective than atenolol to prevent thoracic aortic aneurysm in marfan syndrome through the inhibition of matrix metalloproteinase-2 and -9, Circ. Res. 102 (2008) e73–85.

[42] X. Chen, D.L. Rateri, D.A. Howatt, A. Balakrishnan, J.J. Moorleghen, L.A. Cassis, A. Daugherty, Tgf-beta neutralization enhances angii-induced aortic rupture and aneurysm in both thoracic and abdominal regions, PloS One 11 (2016), e0153811.

[43] K.L. Siu, C. Lotz, P. Ping, H. Cai, Netrin-1 abrogates ischemia/reperfusion-induced cardiac mitochondrial dysfunction via nitric oxide-dependent attenuation of nox4 activation and recoupling of nos, J. Mol. Cell. Cardiol. 78 (2015) 174–185.

[44] J. Ejiri, N. Inoue, T. Tsukube, T. Munezane, Y. Hino, S. Kobayashi, K. Hirata, S. Kawashima, S. Imajoh-Ohmi, Y. Hayashi, H. Yokozaki, Y. Okita, M. Yokoyama, Oxidative stress in the pathogenesis of thoracic aortic aneurysm: protective role of statin and angiotensin ii type 1 receptor blocker, Cardiovasc. Res. 59 (2003) 988–996.

[45] J.A. Phillippi, E.A. Klyachko, JPt Kenny, M.A. Eskay, R.C. Gorman, T.G. Gleason, Basal and oxidative stress-induced expression of metallothionein is decreased in ascending aortic aneurysms of bicuspid aortic valve patients, Circulation 119 (2009) 2498–2506.

[46] E. Kobeissi, M. Hibino, H. Pan, D. Aune, Blood pressure, hypertension and the risk of abdominal aortic aneurysms: a systematic review and meta-analysis of cohort studies, Eur. J. Epidemiol. 34 (2019) 547–555.

[47] F. Cosentino, T.F. Luscher, Tetrahydrobiopterin and endothelial function, Eur. Heart J. 19 (Suppl G) (1998) G3–G8.

[48] S. Kerr, M.J. Brosnan, M. McIntyre, J.L. Reid, A.F. Dominiczak, C.A. Hamilton, Superoxide anion production is increased in a model of genetic hypertension: role of the endothelium, Hypertension 33 (1999) 1353–1358.

[49] U. Landmesser, S. Dikalov, S.R. Price, L. McCann, T. Fukai, S.M. Holland, W. E. Mitch, D.G. Harrison, Oxidation of tetrahydrobiopterin leads to uncoupling of

endothelial cell nitric oxide synthase in hypertension, J. Clin. Invest. 111 (2003) 1201–1209.
[50] J. Vasquez-Vivar, B. Kalyanaraman, P. Martasek, N. Hogg, B.S. Masters, H. Karoui, P. Tordo, K.A. Pritchard Jr., Superoxide generation by endothelial nitric oxide synthase: the influence of cofactors, Proc. Natl. Acad. Sci. U.S.A. 95 (1998) 9220–9225.
[51] R.M. Wever, T. van Dam, H.J. van Rijn, F. de Groot, T.J. Rabelink, Tetrahydrobiopterin regulates superoxide and nitric oxide generation by recombinant endothelial nitric oxide synthase, Biochem. Biophys. Res. Commun. 237 (1997) 340–344.
[52] Y. Xia, A.L. Tsai, V. Berka, J.L. Zweier, Superoxide generation from endothelial nitric-oxide synthase. A ca2+/calmodulin-dependent and tetrahydrobiopterin regulatory process, J. Biol. Chem. 273 (1998) 25804–25808.